# Atmospheric Remote-sensing Infrared Exoplanet Large survey (ARIEL)

# PLM Thermal Analysis Report

## TMM/GMM Description and Results

## Issue 2.0

## ARIEL-INAF-TN-0003

Prepared by: _____ Date: 15.02.2017

D. D'Ascanio (INAF-IASF Bologna),
G. Morgante (INAF-IASF Bologna),
L. Terenzi (INAF-IASF Bologna)
*ARIEL Consortium System Team*

Agreed by: _____ Date: _____

Paul Eccleston *(RAL Space)*
*ARIEL Consortium Project Manager*

Approved by: _____ Date: _____

*Giovanna Tinetti (UCL)*
*ARIEL Consortium PI*

# DOCUMENT CHANGE RECORD

| Issue | Date | Page | Description Of Change | Comment |
|---|---|---|---|---|
| 0.1 | 04-May-16 | All | First draft version of the document | |
| 1.0 | 30-May-2016 | All | General review and TMM results update for MCR | |
| 2.0 | 14-Feb-2017 | All | General update of description and results for MSR | |

# DISTRIBUTION LIST

| ARIEL Payload Consortium | | | | External | |
|---|---|---|---|---|---|
| Co-PIs | | Study Engineering Team Working Group Leads | | European Space Agency | |
| ✓ | Giovanna Tinetti | ✓ | Paul Eccleston | ✓ | Goren Pilbratt |
| ✓ | Giusi Micela | ✓ | Kevin Middleton | ✓ | Ludovic Puig |
| ✓ | Jean-Philippe Beaulieu | ✓ | Emanule Pace | ✓ | Astrid Heske |
| ✓ | Paul Hartogh | ✓ | Gianluca Morgante | | |
| ✓ | Enzo Pascale | ✓ | Tom Hunt | | |
| ✓ | Ignasi Ribas | ✓ | Vania Da Deppo | | |
| ✓ | H. U. Nørgaard-Nielsen | ✓ | Pino Malaguti | | |
| ✓ | Michiel Min | ✓ | Jerome Amiaux | | |
| ✓ | Mirek Rataj | ✓ | Pep Colome | | |
| ✓ | Bart Vandenbussche | ✓ | Jean-Louis Auguères | | |
| ✓ | Manuel Gudel | ✓ | Etienne Renotte | | |
| ✓ | David Luz | ✓ | Martin Frericks | | |
| | | | | | |
| | | | | | |
| | | | | | |
| | | | | | |
| | | Other Engineering Team | | | |
| | | ✓ | *As necessary for doc* | | |
| | | | | | |
| | | | | | |
| | | | | | |
| | | | | | |
| | | | | | |

# TABLES OF CONTENTS

## LIST OF CONTENTS

## LIST OF TABLES

## LIST OF FIGURES

# 1 INTRODUCTION

This living document describes the present status of the thermal analysis of the PLM of the ARIEL mission proposal, candidate for the ESA M4 launch opportunity. A general view of the mission thermal and cryogenic architecture can be found in [RD1]. A general PLM TMM/GMM, both radiative and conductive, has been developed to simulate the main couplings between the SVM boundary and the PLM units in flight representative conditions, to evaluate predicted temperature and loads at internal/external interfaces.

At the beginning of the document the general architecture of the payload is presented. In the following chapters the geometrical and thermal models are described together with the assumptions adopted for simulating the system behavior in terms of radiative and conductive couplings and loads. Finally the main results of the steady-state and transient analyses carried out so far are reported and commented.

At this stage, this model represents the more detailed simulation tool for the ARIEL PLM thermal performances prediction. In future phases of the mission analysis, once the design will be in a more condensed state, dedicated detailed models of single sub-systems (Optical Bench, Instrument Radiator, Telescope Assembly) will be prepared for accurate simulations of the thermal behavior of these PLM units.

This general model will be updated and correlated with the more detailed simulations to provide a reliable representation of the PLM thermal behavior and will be used for general steady-state and transient analyses. It will be maintained, in agreement with ESA and Industry, to become also be the TMM deliverable for representing the ARIEL PLM thermal design inside the general Spacecraft model.

All ARIEL thermal modeling simulations are being developed in the ESATAN-TMS environment.

## 1.1 PURPOSE

This document captures the main information concerning the thermal analysis performed for the ARIEL mission PLM. The purpose is to provide the reader with a comprehensive view of the thermal architecture and of the models developed the mission study of Phase A. The general scheme of the models is reported and explained, including the up-to-date best assumptions and approximations, together with the present knowledge of the boundary conditions. A summary and explanation of the main results presented is also reported.

## 1.2 SCOPE

This document provides an overall summary of the ARIEL PLM thermal analysis activity and TMM/GMM development starting from the mission thermal and cryogenic baseline architecture scheme. It gives an overview of the present status of the thermal models evolving with the mission study process. The best assumptions in terms of heat loads and conductive/radiative couplings are reported with reference to the thermal design. The thermal cases studied and reported in the document are based on the present assumptions of best and worst cases conditions as can be derived from the main mission reference documents [AD1] and [AD3]. A cold and a hot case are run to bound the space phases of the PLM thermal design.

The document shall also be used as a reference for the TMM/GMM, as it describes assumptions, estimations and definitions for the TMM/GMM at the present stage of the study. It is a living document that represents a sort of explanatory note for the G/TMM and thermal analysis updates.

## 1.3 APPLICABLE DOCUMENTS

| AD # | APPLICABLE DOCUMENT TITLE | DOCUMENT ID | ISSUE |
|---|---|---|---|
| 1 | ARIEL Mission Requirements Document (MRD) | ESA-ARIEL-EST-MIS-RS-001 | 1.3 |
| 2 | ARIEL Science Requirements Document (SciRD) | ESA-ARIEL-EST-SCI-RS-001 | 1.3 |
| 3 | ARIEL Payload Interface Definition – Part A (PID-A) | ESA-ARIEL-EST-PL-IF-001 | 0.14 |
| 4 | ARIEL Mission Analysis Guidelines | ESA-ARIEL-ESOC-MIS-AN-001 | 1.1 |
| 5 | ARIEL Payload Requirements Document | ARIEL-RAL-PL-RS-001 | 1.0 |
| | | | |

***Table 1: Applicable Documents***

## 1.4 REFERENCE DOCUMENTS

| RD # | APPLICABLE DOCUMENT TITLE | DOCUMENT ID | ISSUE |
|---|---|---|---|
| 1 | ARIEL Payload Design Description | ARIEL-RAL-PL-DD-001 | 2.0 |
| 2 | ARIEL PLM Harness Thermal Analysis | ARIEL-INAF-PL-TN-0005 | 1.0 |
| 3 | Margin philosophy for science assessment studies | SRE-PA/2011.097/ | 2.1 |
| 4 | AIRS Design Description | ARIEL-CEA-INST-DD-003 | 1.1 |

***Table 2: Reference Documents***

# 2 SYSTEM THERMAL DESIGN

## 2.1 BASELINE THERMAL ARCHITECTURE AND DESIGN

The spacecraft thermal design (Figure 1) is based on a cold Payload Module (PLM) sitting on the top of a warm Service Module (SVM) (see [RD1]). The mission thermal control is accomplished by a combination of passive and active cooling systems. The SVM is thermally controlled in the 270K-290K range for nominal operations of all the S/C subsystem units. The function of the cold PLM is to shield the scientific instrumentation (the ARIEL instrument and the telescope system) from the warm section of the S/C and to provide it with the required cooling and thermal stability.

Passive cooling is achieved by a high efficiency thermal shielding system (Figure 1 and Figure 2) based on a multiple radiators configuration that, in the L2 environment, can provide stable temperature stages down to the 50 – 60 K range. At 1.5 million km from the Earth in the anti-Sun direction, the L2 orbit allows to maintain the same spacecraft attitude relative to the Sun-Earth system, while scanning the whole sky during the mission duration. Limiting the allowed Solar Aspect Angle (SAA) range, ARIEL will operate in a very stable thermal environment keeping always protect from the Sun/Earth/Moon illumination the coldest section of the PLM. For this reason the SAA allowed during nominal observations will be limited to ±5° around the S/C X-axis and to ±25° around the Y-axis. An extra margin due to possible contingencies, respectively of 1° and 5°, has been assumed on these values: the thermo-mechanical architecture of the PLM has been designed within a total envelope of ±6° around the spacecraft X-axis and ±30° around the Y-axis (Figure 3).

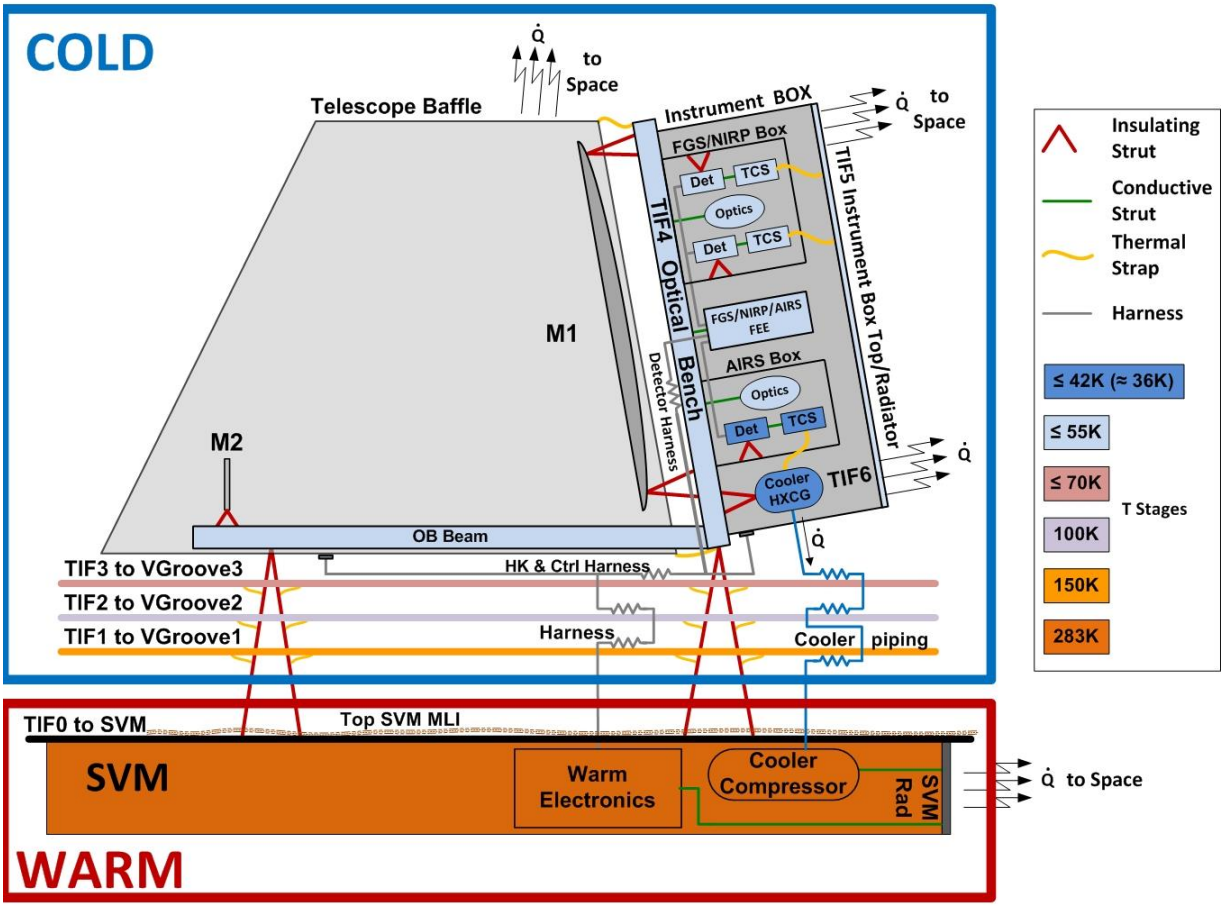


***Figure 1: PLM thermal Architecture Scheme***

The SVM upper surface, the main thermo-mechanical interface of the PLM to the S/C, is covered with a low emissivity MLI shroud and acts as the first main radiative barrier between the PLM and the warm units in the service module. The geometrical configuration of the PLM passive stages and the maximum Solar Aspect Angles allowed during the mission are strongly related. The SVM interface is assumed, at this stage of the study, as a perfect Sun shield for the PLM in the thermal analysis. This assumption will be verified in the next

thermal analysis and design steps as the first Sun shielding stage and the PLM passive cooling system must be mutually designed.

The passive cooling system is based on a three V-Grooves combination (Figure 1 and Figure 2). They represent the first cooling stage of the PLM. Mechanically supported on the SVM by bipods and other insulating struts, their shape, geometrical configuration and optical properties allow an efficient rejection of heat to cold space (Figure 3). Past missions (such as Planck, Spitzer Telescope and Herschel) have demonstrated that, in an environment such as L2, is possible to passively reach and maintain temperatures down to the 50K range with loads up to more than 1W. These three radiators, called V-Groove 1, 2 and 3 (VG1, VG2, VG3), work in sequence at temperatures around 190K, 120K and 60K respectively, providing stable temperature references for the Instrument units, for parasitic heat leaks (harness, struts, radiation) interception and for cryo-cooler pre-cooling. The last V-Groove, VG3, defines the coldest passive environment of the PLM and accommodates the Instrument modules and the Telescope Assembly (Figure 2).

The V-Grooves structure, light but rigid, is composed of an Al sandwich with an internal honeycomb structure. The thermo-optical efficiency of this radiators system relies on angled highly-reflective surfaces open to space, rejecting radiation after a number of reflections between the angled shields (see Figure 3). Only the upper surface of the third radiator (V-Groove 3), always exposed to deep space during operations, is coated with a black painted honeycomb structure to maximize heat rejection.

The telescope is required to operate at a temperature <70K. The Telescope Assembly (TA), enclosed in the cold environment established by the last V-Groove, acts as an extra passive stage using its large Baffle and Optical Bench (TOB) as radiating surfaces. These radiators, all arranged in the same black painted open honeycomb structure configuration, greatly improve the efficiency and the performances of the PLM passive cooling.

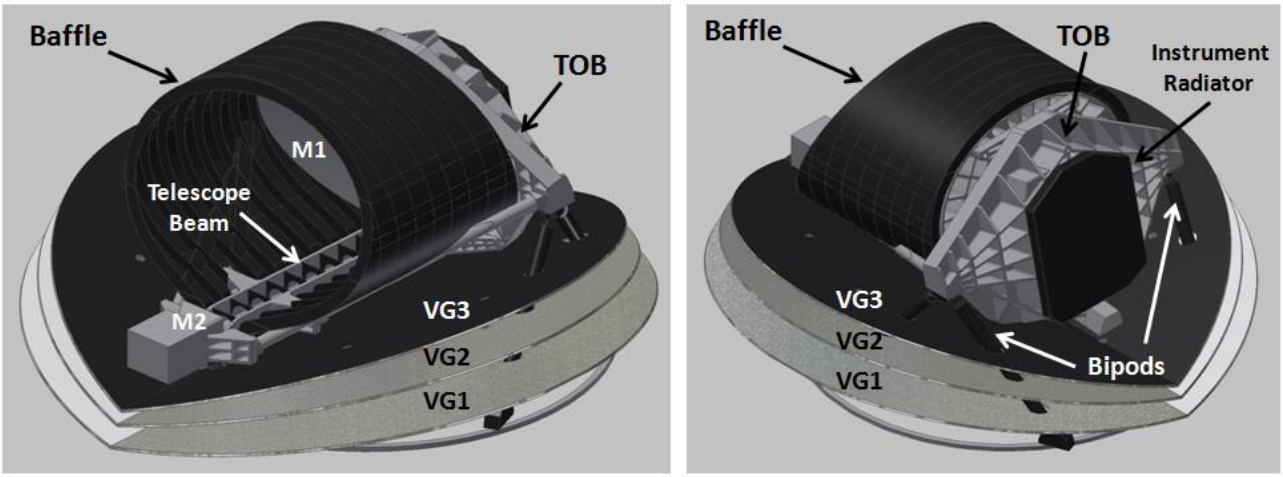


***Figure 2: ARIEL PLM thermo-mechanical architecture***

The ARIEL Instrument modules are integrated on the Optical Bench and their cooling is achieved in two different ways, following the different temperature requirements of each frequency band. The detectors of two channels, the Fine Guidance System (FGS) and the Near Infrared Photometer (NIRP), located in a single module box (the FGS box) are passively cooled to T ≤ 70K by a dedicated radiator represented by the top surface that closes the modules cavity on the Optical Bench. This radiator, fully enclosed in the cold radiative environment set by the last V-Groove, always faces the cold space during operations. The ARIEL Infra-Red Spectrometer (AIRS) detectors must be operated colder, below 42K (see Table 3), with the goal of reaching a temperature around 36K, to minimize detector noise. Maintaining this temperature, with a load of tens of mW, require the implementation of an active cooling system. The cryocooler baseline relies on the Planck mission and EChO study heritage: a JT cold end fed by a Planck-like mechanical compressor using Neon gas isenthalpic expansion to achieve the required low temperature and heat lift (see [RD1]). The design of the ARIEL active cooling system is under the responsibility of the Rutherford Appleton Laboratory (RAL) in the UK.

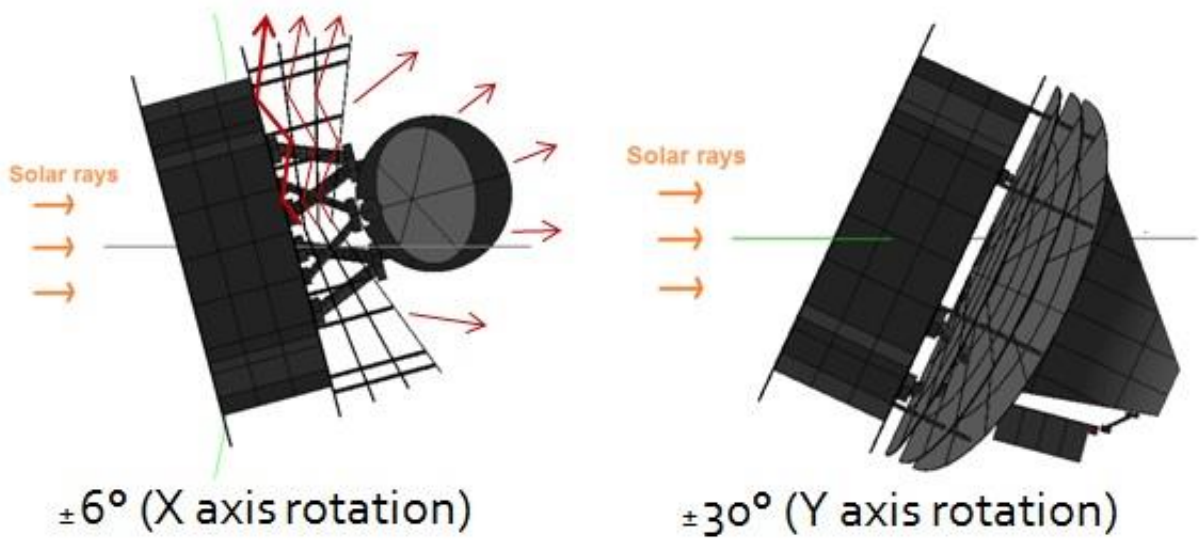


***Figure 3: ARIEL S/C attitude and SAA in orbit***

The general scheme of the PLM, shown in Figure 1, indicates the six main thermal interfaces of the PLM identified in the analysis. The design of the PLM thermal architecture is driven by the required operating temperature of each unit and interface, in combination with the expected loads at the thermal stages. These values are reported in the following Table.

***Table 3: Main thermal requirements and expected loads for the ARIEL payload***

| ARIEL PLM thermal requirements | | | Thermal Interface (TIF) temperature and expected load[1] [mW] | | | | | | |
|---|---|---|---|---|---|---|---|---|---|
| | | | SVM (TIF 0) | VG1 (TIF1) | VG2 (TIF2) | VG3 (TIF3) | TOB/BAF (TIF 4) | Instr. Rad. (TIF5) | JT CE (TIF 6) |
| | | | T_Op [K] | T_Op [K] | T_Op [K] | T_Op [K] | T_Op [K] | T_Op [K] | T_Op [K] |
| **Payload Unit** | **T_Op [K]** | **ΔT[4] [K]** | 280[2] ± 10<br>190[3] ± 10 | ≤ 180 | ≤ 120 | ≤ 70 | < 60 | < 60 | < 40 |
| **Telescope** | < 70 | ± 1 | - | - | - | - | TBD[5] | - | - |
| **FGS / NIRP Optics** | ≤ 60 | ± 0.5 | - | - | - | - | - | - | - |
| **FGS detector** | ≤ 70 | ± 0.1 | - | - | - | - | - | 20[6] | - |
| **FGS CFEE** | ≤ 70 | ± 2 | - | - | - | - | 100[7] | - | - |
| **NIRP detector** | ≤ 70 | ± 0.1 | - | - | - | - | | 20[6] | - |
| **NIRP CFEE** | ≤ 70 | ± 2 | - | - | - | - | 100[7] | - | - |
| **AIRS Optics** | ≤ 60 | ± 0.5 | - | - | - | - | - | - | - |
| **AIRS detector 0** | ≤ 42 | ± 0.05 | - | - | - | - | - | - | 15[6] |
| **AIRS detector 1** | ≤ 42 | ± 0.05 | | | | | 100[7] | | 15[6] |
| **AIRS CFEE** | ≤ 62 | ± 2 | - | - | - | - | 100[7] | - | - |
| **Parasitic leaks[1] (struts + harness + piping + radiation)** | NA | NA | -10000 | TBD[8] | TBD[8] | TBD[8] | 50 | 10 | 5 |
| **Total load[1] (no margin) [mW]** | | | -10000 | TBD | TBD | TBD | 450 | 50 | 35 |
| **Total load[1] (w/ 50% margin) [mW]** | | | -15000 | TBD | TBD | TBD | 675 | 75[9] | 53 |

*Notes:* [1] *Based on thermal analysis of present PLM design*

[2] *Conductive interface to SVM*

[3] *Radiative interface to SVM*

[4] *Peak to peak value over a typical observation time (7 hours)*

[5] *M1 thermal control system dissipation, if needed, is expected to be < 2W*

[6] *FPA loads estimated with margin. The AIRS numbers already include the contribution of the FPA support and harness; ~5 mW are the allocated for temperature control*

[7] *Worst Case dissipation*

[8] *To be evaluated by thermal analysis*

[9] *Radiator with A ≥ 0.3 $m^2$ radiator*

Besides the third V-Groove, the two main PLM radiators are the instrument cavity cover and the Telescope Baffle. The baseline design of their external surfaces is based on a black painted open honeycomb cell structure to maximize IR emissivity ($\varepsilon \geq 0.9$). Instrument radiative thermal control is achieved by properly selecting the thermo-optical properties of the exposed surfaces. The radiative environment for the modules is set by the Optical Bench cavity and the Instrument Radiator that shield the channel modules and the common optics from the external environment. The remaining surface of the OB, directly exposed to cold space, is black painted (TBC). The internal surface of the bench cavity that accommodates the instrument modules and optics requires a black coating to minimize optical stray-light leaks (TBC). For the same reason, the module boxes are assumed externally treated with black paint or high emissivity coatings.

In general, most of the ARIEL PLM units require high emissivity coatings to maximize passive cooling performances. As anticipated in the present issue of the Mission Analysis Guidelines document, there is the possibility of Sun intrusion in the PLM after launch, during the LEOP (TBC). For this reason transient simulations have been carried out with the TMM to evaluate the impact of direct solar illumination on the most sensitive units (detectors and optics). The preliminary results indicate that the temperature of these units is not rising to dangerous values if the exposure is limited to periods not longer than 60 minutes. The thermal inertia of the PLM helps in keeping the internal temperature within a safe range. If prolonged Sun exposures will be predicted a different approach for the thermo-optical design of radiating surfaces may be required. A possible alternative could be represented by flat surfaces (no open honeycomb structure) coated by lower solar absoprtance layers such as white paint.

The FGS/NIRP and the AIRS modules share a similar thermal design (see Figure 5). Both channels are integrated in a box that includes optical elements and a detector assembly, composed by the Focal Plane Assembly (FPA) and the cold front end electronics (CFEE). Due to electrical performance issues the cryo-harness connecting the Cold Front End Electronics (CFEE) to the detectors cannot be longer than 10 - 15 cm max. From this follows that the CFEE shall be mounted on each module box in proximity of the detectors working at the same temperature of the Optical Bench units. By tuning their thermal coupling to the OB it could be possible, if needed for performances optimization, to use their internal dissipation to keep them at a slightly higher temperature. CFEE loads are finally rejected to space by the main radiator stages.

The FGS and NIRP channels are integrated in a single Module Box and work in the same temperature range, with the optical units and the detectors at a temperature, respectively, ≤ 60K and ≤ 70K. For the detectors Focal Plane Assembly (FPA) the general rule is the colder, the better. For this reason the detectors are cooled by a dedicated passive radiator stage, the Instrument Box top face (TIF5 in Figure 1) located inside the cold environment set by the third V-Groove and the Telescope Assembly. This radiator is mechanically supported on the Instrument Box by means of insulating supports and is under Instrument Consortium responsibility. The FGS and NIRP detectors are thermally decoupled from the Module Box and high conductive links connect them, through their thermal control stages, to this radiator. The Module Box of the FGS and NIRP channels is thermo-mechanically linked to the bench by means of a conductive interface. In this configuration, at steady state, the FGS/NIRP optical units are expected to thermally equilibrate with the Optical Bench.

The AIRS detectors technology baseline requires lower operating temperatures, on the order of 40K (T ≤ 42K with a goal of 36K), to achieve the required sensitivity. This temperature is reached by using the Ne JT cooler, capable of producing a heat lift up to of 50 mW or more. The AIRS module optics shall operate at a temperature similar to the other channels, 60K or below. For this reason, while the AIRS Module Box is thermally coupled to the OB, the FPA needs to be carefully insulated from the box, to limit the heat leak to the JT cooler cold end. In order to provide the required cooling to the AIRS detectors, the cold end heat

exchanger is located in proximity the FPA, to minimize the thermal link distance, and supported on the Optical Bench by insulating struts.

In general, each detector stage is thermally decoupled from the relative module box, to maximize performances of the FPA in terms of absolute temperature and stability. Coupling to the temperature reference stage is achieved through a Thermal Control Stage (TCS): this is an active closed loop thermal control system composed by a heater + thermometer couple driven by the ICU/TCU and located on the SCA's frame. The thermal control stage of each detector is then directly coupled to the relative reference temperature stage (JT cold end or instrument radiator) by means of high conductivity thermal straps made by high purity Aluminum.

The warm electronics and cooler compressor are located in the SVM. All harness and piping from SVM to Instrument channels should be thermally linked to all passive stages (VG1, VG2, VG3) to minimize parasitic leaks on the instrument cooling stages. In particular, cryo harness heat leaks to detectors shall be controlled by thermally optimizing the cables design with respect to the required electrical performances (see Chapter 2.3.7).

## 2.2 THERMAL INTERFACES DEFINITIONS

In the ARIEL PLM thermal architecture seven main Thermal Interfaces (TIF's) have been identified (see Figure 1): one to the S/C and the others internal to the PLM. The system thermal design has been based on the flow down of the basic instrument requirements (Table 3) to the main thermal interfaces (Table 4). The IF temperature values are fixed by the detectors/optics operating point and by the assumed total conductance from these units to their interfaces. The thermal stability requirements of the interfaces over a typical exposure time is set to ensure the required stability of the module units. The stability across longer periods, such as seasonal or orbital changes over mission, must be taken into account when dimensioning the interfaces and the relative couplings. The requirements in Table 4 are defined to ensure best thermal performances of the optical and detector systems over longer periods and full mission lifetime.

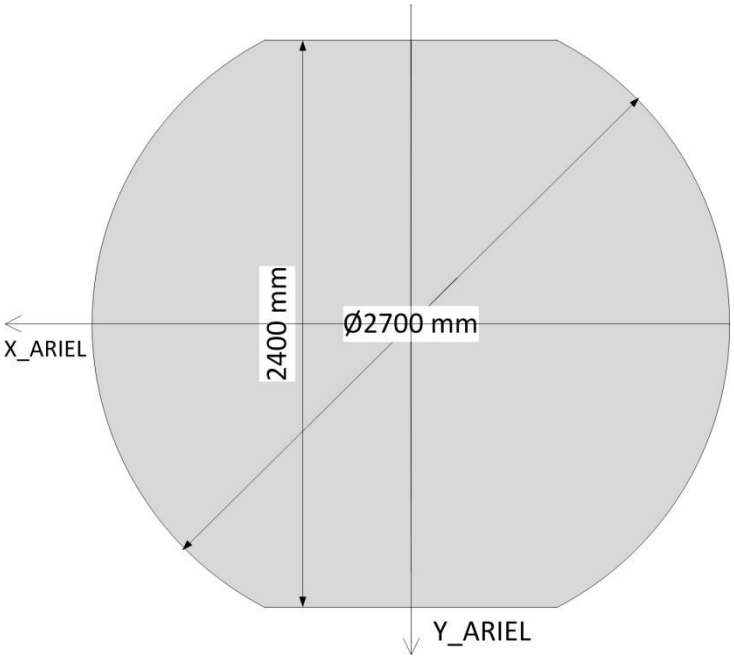


***Figure 4. SVM thermo-mechanical interfaces dimensions***

The PLM interface to the SVM is the S/C platform: a 2700 mm circular surface cut in the Y axis direction at a distance of 2400 mm from the X axis (Figure 4). For thermal analysis purposes this platform is assumed as split in two interfaces: a conductive plate and a MLI radiative shroud. The platform is considered, for both interfaces, a fixed boundary, fully shielding the cold PLM from Sun and warmer section of the S/C, with the following characteristics:

- Conductive coupling:
  - temperature range 270 – 290K
  - stability over an observation period +/- 3 K over 10 hours
- Radiative coupling:
  - IR emissivity = 0.05
  - temperature range 180 – 200K with stability over an observation period +/- TBC K

All conductors linking warm units in the SVM to the PLM are considered coupled to this interface (including harness and cooler piping) but the main conductive couplings of the PLM with this interface are the bipods and V-Groove struts. The contact surface of each bipod foot is around 50 $cm^2$ (for the struts $A_c \approx 5$ $cm^2$) and the assumed surface contact conductance for these couplings is 800 $W/m^2$-K, a conservative value for bare interfaces (no thermal filler) with A < 100 $cm^2$.

For a cryogenic instrument, internal and external thermal interfaces are the key to a successful design. The detectors must be thermally decoupled from the OB, by resistive supports to improve their stability, while thermal contact with the cooling stage (JT cold end or cold radiator) must be maximized. This requires that the cooler cold end is located nearby the AIRS module to minimize the thermal path of straps (see Figure 5). The JT cold tip is mounted at a convenient position on the Optical Bench by means of insulating supports. The Instrument Radiator is integrated on the Optical Bench through insulating connection points. Presently, the allocated area for this radiator is defined by the dimension of the open cavity that encases the instrument modules, but there is still margin to increase its size, if needed. High conductivity thermal straps are used to connect the FGS/NIRP and AIRS channel detectors to their operating temperature reference, respectively the Instrument Radiator and the JT cold heat exchanger.

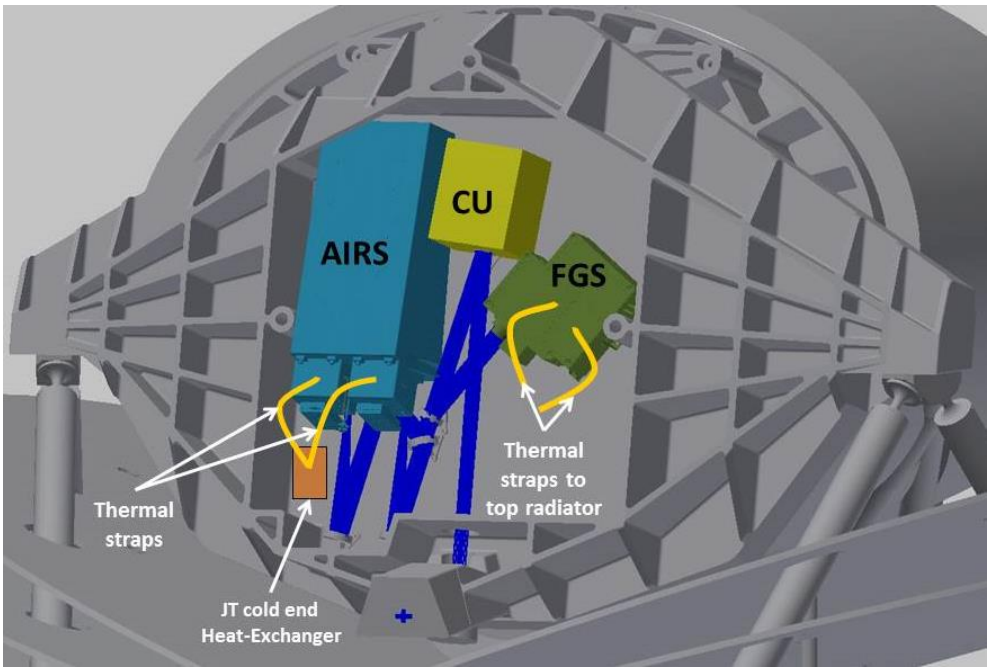


***Figure 5: Modules thermo-mechanical configuration on the OB***

The required conductance across each thermal interface is evaluated by analysis running thermal model simulations (see Chapter 3.3). A typical value of 500 $W/m^2$-K is assumed as the average surface thermal conductance of machined metallic interfaces in the temperature ranges expected for the ARIEL PLM. This value was achieved with enough margin in several Planck couplings in the 20-55K range, based on M4 bolts, using spring washers and, in some cases, a filler (gold sheet). The required conductance values and limits at the ARIEL TIF's have been bounded and checked by running preliminary parametric analysis. A justification of the assumptions made on the main conductive links is reported in the Technical Note describing the TMM/GMM. The high level specifications of the thermal couplings of PLM units to the main interfaces are summarized in the following table. The values refer to a single coupling.

***Table 4: TIFs main requirements***

| I/F | Unit | I/F to | T (K) | ΔT[1] (K) Vs time | G across IF (W/K) | Contact Area ($cm^2$) |
|---|---|---|---|---|---|---|
| TIF0 | SVM | SVM top platform | < 290 | < ± 3 | < 10 | < 100 |
| TIF1 | VG1 | Warm Harness, cooler piping | ≤ 180 | ≤ ± 3 | ≥ 0.5 | ≥ 10 |
| TIF2 | VG2 | Warm Harness, cooler piping | ≤ 120 | ≤ ± 1 | ≥ 0.5 | ≥ 10 |
| TIF3 | VG3 | Warm Harness, cooler piping | ≤ 70 | ≤ ± 1 | ≥ 0.5 | ≥ 10 |
| TIF4 | TOB/Baffle | Modules, CFEE, Mirrors, Harness | ≤ 60 | ≤ ± 1 | ≥ 0.5 | ≥ 10 |
| | | Telescope mirrors | | | < 0.1 | < 100 |
| | | Detectors FPA | | | < 0.001 | < 2 |
| | | JT cold end | | | < 0.01 | < 5 |
| TIF5 | I Radiator | FGS/NIRP detectors | ≤ 60 | ≤ ± 0.1 | ≥ 0.1 | ≥4 |
| TIF6 | JT cold end | AIRS detectors | < 40 | ≤ ± 0.1 | ≥ 0.1 | ≥2 |

*Notes: [1] Peak to peak value over a typical observation time (10 hours)*

Each detector FPA is supported on a flange that works as the active Thermal Control Stage (TCS) by thermally dimensioned supports to achieve a tuned thermal break. TIF5, for FGS and NIRP detectors is located on the back side of the radiator. TIF6, for the AIRS FPA, is the JT cold end heat exchanger, supported on the bench by insulating struts and is located in proximity of the spectrometer box side where the detectors are positioned. The assumed contact area is 2 $cm^2$.

The conductance values defined in this study, and assumed for the thermal analyses, can be achieved using standard materials and solutions adopted already in previous experiments (e.g. MIRI and Planck): GFRP for insulating struts (Ti alloy can be used for specific fixtures) and 5N Al (or Cu) for the high conductivity links. Standard Al alloys (such as 6063 or 6061) are used for most of PLM structures and units as well as for the telescope structure. Stainless steel (TBC) bolts (A2-70) not smaller than M4 shall be used for the main mechanical couplings to Spacecraft and to the TOB. In general, to optimize the thermal contact, the maximum bolt dimension allowed by the mechanical allocations and design should be used. If needed, spring washers and a thermal filler (Gold or Indium foil for example) could be considered to improve conductance.

## 2.3 PAYLOAD MODULE THERMAL CONTROL HARDWARE

The ARIEL Thermal Control Hardware (TCHW) includes all passive or active components that are used to reach and maintain the operating temperatures of the PLM units within their required ranges.

The high level list of the PLM TCHW items is composed by:

- V-Grooves (including bipods and struts)
- Instrument Radiator (top face of the box)
- Telescope Baffle (upper half)
- Thermal straps
- Thermistors (monitoring and control)
- Detectors temperature control stage (TCS)
- Telescope Mirrors temperature control stage
- Heaters

The first five items are fully passive components while the other three can be considered part of the active thermal control system.

### 2.3.1 V-Grooves

V-Grooves (VG's) design is a key issue of the ARIEL thermal performance as they represent the first cooling stage of the PLM. VGs are high efficiency, passive radiant coolers, whose performances in a cold radiative environment such as L2 has been definitely demonstrated by the Planck mission. ARIEL V-Grooves system consists in a set of three specular shields, composed by six half circles arranged in a "V-shaped" configuration, angled along the diameter parallel to the S/C X axis (Figure 6). Their objective is to intercept radiative and conductive heat leaks from warmer sections of the S/C and spread it away to deep space after multiple reflections between each VG pair. Each VG shield is tilted by a certain angle with respect to the adjacent one, creating a divergent radiative path for the reflected thermal rays. Figure 6 shows a simplified schematic of this concept. In the present thermal configuration the three VG angles are 10°-15°-20°.

The thermo-optical properties of the VGs are of essential importance since they are the key parameters for thermal isolation and heat rejection to space. To achieve the required performances, VGs surfaces must have a very low emittance coating, a high reflection/mirroring material needed to reflect heat radiation. A 3N pure aluminum coating with a Vapor Deposited Aluminum (VDA) can reach an emissivity in the IR band of less than 0.05, as measured on the Planck PLM. The upper surface of the last VG (VG3), exposed to the cold sky, is covered by an open aluminum honeycomb structure coated with high emissivity black paint (MAP® PUK, or Aeroglaze Z306) to maximize the radiative coupling, and so heat rejection to deep space.

The bipods (Figure 7) and V-Grooves struts are hollow tubes made of GFRP (R-glass + epoxy), with rigid foam inside to increase their mechanical performances while limiting thermal conductance across the stages. The rear bipod legs are 620 mm long, with a diameter of 50 mm and a thickness of 5 mm. The pod feet are made of Al alloy with Ti alloy (Ti6Al4V) fixtures. The smaller front bipod legs are 220 mm long, with a diameter of 30 mm and a thickness of 3 mm. During flight operations all bipod legs will always face the cold sky so their external surface is black painted to maximize self heat rejection to space. This configuration ensures a very limited heat leak through the length ($G < 10^{-4}$ W/K).

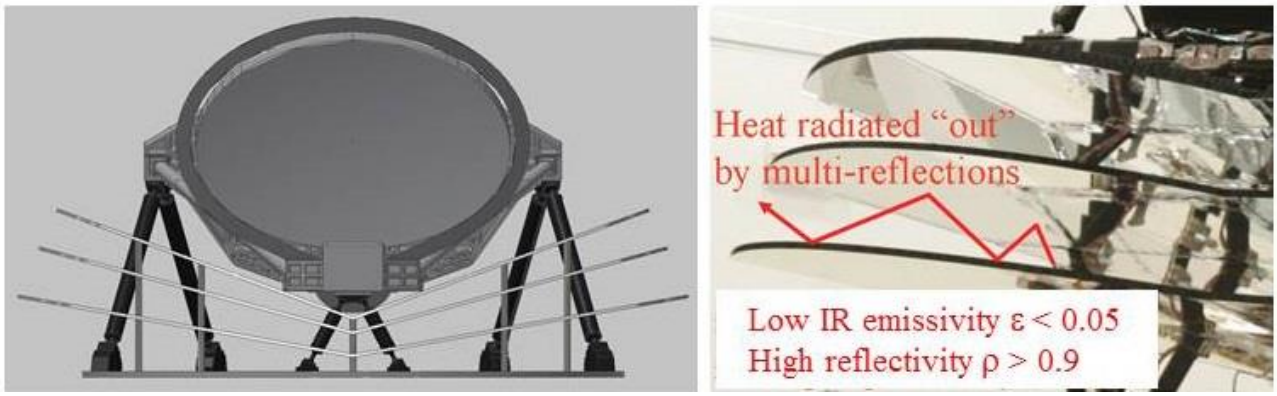


***Figure 6. ARIEL V-Grooves scheme***

Even if bipods and struts are good thermal insulators, to minimize heat leaks to the PLM colder stages, they must be thermally coupled to the V-Grooves. Each mechanical support is connected, by means of at least two thermal straps, to each VG as shown in Figure 7. For further parasitic loads reduction all bipods and struts are black painted to increase self-rejection to space. For the same reasons, the harness from the warm electronics in the SVM to the cold units is thermally coupled to each VG in order to reject its conductive load. The JT cooler piping dissipates the gas pre-cooling load on the V-Grooves by means of heat exchangers located on the shields. As a conservative case for the thermal analysis we have considered the harness interception load on VG3 and a pre-cooling power of 320mW entirely dissipated on one node of the last VG only. Even in these conditions, a thickness of less than 1 mm of the Aluminum skin is sufficient to limit the temperature gradient over the shields to less than 3K between the hot spots (cooler & harness heat exchangers) and the rest of the panel.

### 2.3.2 Telescope Baffle and Instrument Radiator

The V-Groove-based design provides a cold and stable environment for the PLM units: telescope, instrument and cryocooler cold end. In this volume all main surfaces exposed to cold space can work as radiating units to increase margins and performances of the PLM passive design. For this purpose the main surfaces are the Instrument Radiator (the top face of the Instrument Box) and the top half of the Telescope Baffle. Potentially also the exposed areas of the Optical Bench or the side walls of the Instrument box can help in this direction and it is assumed that all these surfaces will be coated by a high IR emissivity layer (black paint, MAP® PUK, or Aeroglaze Z306).

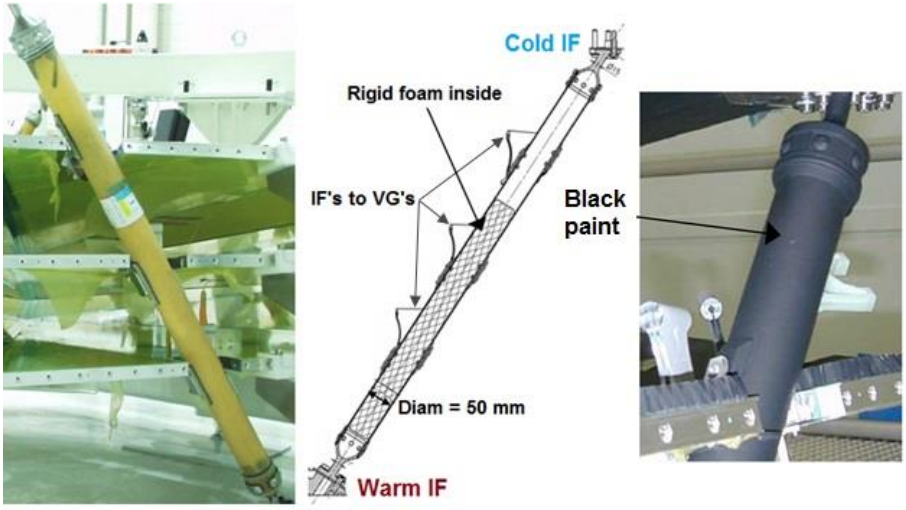


***Figure 7. Bipods configuration***

The top half of the Telescope Baffle will always directly face the cold sky during nominal operations and, given its large surface, offers a great chance of improving the passive performances of the ARIEL S/C. For this reason the surface shall be optimized in terms of IR emissivity: at present the Baffle is designed as a black painted sandwich of Al6061 alloy layers. A honeycomb cell structure 12 mm thick, with 10 mm cell size and ribbon thickness of less than 0.1 mm on the external surface, supported on a 1 mm thick skin (see Figure 8). The internal surface of this skin, that faces the telescope cavity inside the baffle, is black painted also for stray-light control purposes.

This thermo-mechanical design reduces mass while ensuring at the same time a very good thermal conductance in all directions and mechanical stiffness. The baffle has a mass of ~10 kg and is mechanically supported on the two stiffening arms of the telescope structure close to the middle position along its main axis. In this way thermo-elastic contraction will not apply stress to any other unit. The baffle is also thermally connected with high conductance straps to the Optical Bench itself to provide a single large passive stage (TIF4) for all instrument units. If it will be required to support the Baffle also on the OB, elastic mountings will be designed. These extra supports could replace or integrate the thermal straps.

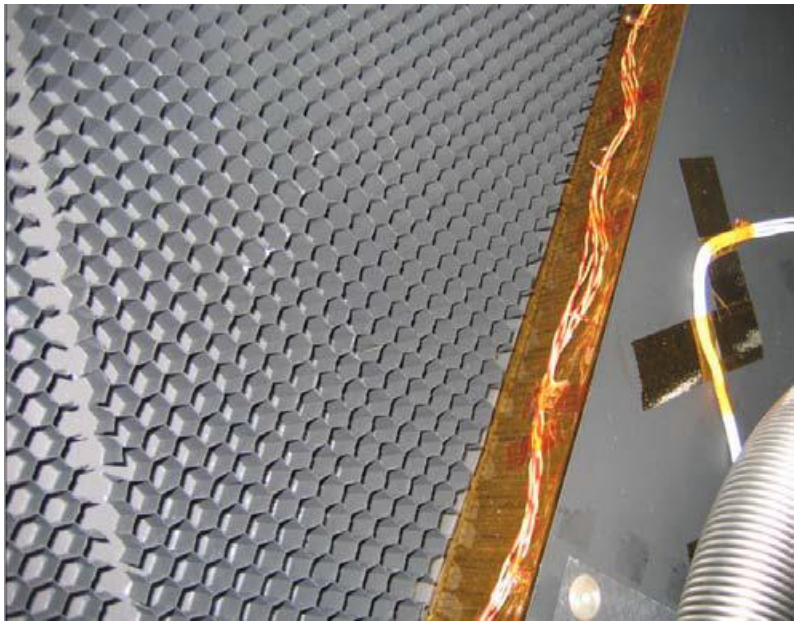

***Figure 8: Example of Planck Baffle thermo-optical configuration***

The top face of the Instrument Box is used as a dedicated radiator for detectors (TIF5). The FGS and NIR Photometer channel requirements (see Table 3) in terms of operating temperature, stability and dissipated loads need a cold radiator dedicated to detectors cooling only. This extra passive stage, called Instrument Radiator (IRad), like the Telescope Baffle, is designed and developed under the responsibility of the Consortium. The radiator is mounted directly on the optical bench, covering the cavity that accommodates the channel modules, by means of insulating supports. Even if the operating temperature of the radiator will be very similar, if not equal, to the TOB and baffle, this configuration would decouple the radiator from any possible instability generated by components functioning in the Box, helping the thermal control process of the FGS channels FPA. In this way the radiator is fully devoted to cool the channel detectors, with parasitic leaks due only to its own supporting struts and thermal monitoring harness. The expected active load due to detector stages is around 30 mW. The conductive load on the radiator due to struts and harness is estimated to be less than 10 mW. In total, 75 mW (including 50% margin) is the expected load to the cold radiator, in the worst case.

At present, the Instrument Radiator approximated dimensions are 600 mm x 635 mm, with a top face area around 0.37 $m^2$, with the exposed surfaces of the Optical Bench contributing for an extra 0.3 $m^2$. In case a larger margin is needed, a wider surface (in the 0.4 – 0.5 $m^2$ range) of the Instrument Box top could be easily fit in the allocated volume on the bench if needed. The radiator orientation is parallel to the OB with an angle around 12° with respect to the vertical direction. The optical properties of the IRad are the same of the Telescope Baffle as the outer surface is based on the same radiative configuration: a 12 mm thick black painted honeycomb cell structure of Al6061 alloy, 10 mm (or less) cell size and ribbon thickness of 0.1 mm mounted on 1 mm thick skin. As demonstrated by Planck, this thermo-optical configuration is capable of rejecting more than 300 mW per square meter in L2 orbit. The ARIEL G/TMM results seem to confirm this assumption. The internal surface of the radiator is, at this stage, assumed to be black painted due to stray-light control. A low emissivity coating, if acceptable, may help in gaining some more margin on the radiator performances, in case is needed, by limiting possible radiation loads from the warmer parts of the OB.

### 2.3.3 Thermal straps

The main conductive links of the ARIEL PLM units are based on high purity 5N Al braids (wires or foils). Because of the high thermal conductivity of pure Al at low temperatures, and its low density, it is possible to maintain dimensions, and mass, of the braids within allocations. The thermal straps are used to connect:

- the bipods to the VGs for conductive parasitic leaks interception: one (or two) straps per bipod leg per VG;
- the Telescope Baffle to the Optical Bench: four straps;
- the channels FPA's to their temperature reference (radiator or cooler cold end): one per detector.

The total conductance across a strap is the combination in series of conductance through the flanges and braids. In the 40-60 K range, the average conductivity of high purity Al (5N) is around 1000 W/m-K. The total conductance of a metallic braids thermal link is commonly assumed to be

$$G_{braid} = \frac{kA}{L} \cdot \eta_p \eta_s \eta_e$$

where η indicate efficiency factors that take into account realistic inefficiencies in the density of wires (or foils) per unit area, in the effective length of the link (due to turn and bends) and in the welds of the braids to the end flanges. Assuming typical conservative values for these factors and imposing a safe estimation of the distance between the units, it is possible to evaluate dimensions and mass of the braids required to achieve the required G across each link.

***Table 5. ARIEL thermal braids preliminary dimensions***

| Units | Total G (W/K) | N of straps | Length (m) | Effective Length (m) | Section ($cm^2$) | End flanges dim (cm) | Tot mass (g) |
|---|---|---|---|---|---|---|---|
| Bipods | ≥ 0.2 | 18 | 0.05 | 0.1 | 34.8 | 20x20x3 | 291 |
| Tel Baffle | > 1.0 | 4 | 0.2 | 0.25 | 755.9 | 40x40x3 | 2219 |
| FGS Det | ≥ 0.1 | 1 | 0.3 | 0.35 | 58.2 | 20x20x3 | 63 |
| NIRP Det | ≥ 0.1 | 1 | 0.3 | 0.35 | 58.2 | 20x20x3 | 63 |
| AIRS Det | ≥ 0.1 | 1 | 0.2 | 0.25 | 41.6 | 20x20x3 | 35 |
| | | | | | | Total mass (g) | 2671 |
| | | | | | | Total mass with margin (50%) | 4006 |

### 2.3.4 Thermistors

The ARIEL number and specifications of the thermometers have been defined on the basis of the present knowledge of the PLM units and TIF's design. Detailed temperature monitoring is achieved by the combination of direct measurements with units thermal prediction analysis, correlated with all ground test results at sub-system and system level.

For the instruments units and the cooler cold end monitoring, Cernox sensors are the baseline (TBC). For the telescope and other PLM units (such as the V-Grooves) PRT's or diodes can be used, using Cernox only for thermal control purposes (mirrors, critical interfaces etc.). On large surfaces (benches, M1), when thermal gradient need to be monitored with accuracy, thermocouples may become a possible alternative to reduce the number of thermistors.

A preliminary selection indicates the following types:

- Cernox 1050-1070
- DT-670 Silicon diodes
- PT100 PRT

The full number of sensors needed to monitor the PLM from the ICU/TCU in flight has not been finally defined yet. This number must be kept as low as possible in order to minimize the number of wires and harness complexity. At the same time the thermistors shall be enough to ensure, in combination to the units thermal mapping resulting from the correlated TMM, a complete monitoring of the PLM during flight operations. A thermometer is installed in correspondence of each TRP, main thermal interface or critical

item. At this stage, all thermistors are assumed to be fully redundant, with the backup items connected to the redundant ICU/TCU.

The readout/acquisition rate of the temperature of critical items (detectors, control stages, cooler cold end, etc.) shall be 1 Hz. The fully passive units (such as the V-Grooves, the Baffle, the Bench) can be monitored at a relaxed rate (with periods of tens of seconds), especially if they result dominated by low frequency variations. All thermistors reading shall be based on 4-wires measurement with connections to the readout electronics arranged in shielded twisted pairs to minimize EMI from external sources.

A resolution of at least 20 mK and an accuracy of 50 mK are required for the PLM units when they are in their operational range. The thermistors used for detectors thermal control should have a resolution of at least 10 mK for the detectors and 100 mK for the M1 in a narrow (few K) range around the operating temperature.

A first estimation based on the present design can be provided (TBC):

- 26 nominal (+26 redundant) Cernox sensors
- 20 nominal (+20 redundant) diodes or PRT

In summary, a total of nearly 50 sensors shall be acquired by the ICU/TCU (TBC): approximately 60% of them will be read at 1Hz frequency while the remaining at a slower rate (TBD).

Extra thermal sensors may/will be integrated on the PLM by the spacecraft Prime Contractor but these will be monitored by the S/C electronics and will not be under Consortium responsibility.

The preliminary evaluation of thermal sensors for PLM monitoring is summarized in Table 6.

### 2.3.5 PLM active thermal control system

One of the tasks of the ICU/TCU is the thermal control needed to stabilize the units during normal scientific operations. The process is based on reading the PLM thermistors and controlling the heaters according to the general specifications summarized in this chapter.

All other thermal control operations such as decontamination and survival are, at the moment, considered under S/C responsibility. Thermal monitoring for these procedures will be based on thermistors that are part of the S/C. In this way the two thermal monitoring/control chains (S/C and PLM) are considered independent, each responsible of the relative sensors/heaters.

The PLM units that may require active control are the telescope mirrors and the detector focal planes. At this stage of the design, it is assumed that the primary mirror M1, the secondary M2 and M3 shall be actively controlled. The instrument channel detectors require active thermal control, as the stability requirement is demanding.

Thermal control is based on a feed-back loop, Proportional-Integral-Derivative (PID) type controller, operated with a frequency rate of 1Hz (TBC) as the relevant fluctuations expected on the controlled units should have typical time periods much longer that 1 second. All possible faster fluctuations, for example cooler compressor induced (around 40 Hz, TBC) if relevant, are filtered out passively by the thermal inertia of the units. Controlling every second will allow to respond efficiently to all expected oscillations. Each control loop should be able to read the temperature and adjust heater power, if needed, within a 1s cycle.

All thermal control stages are assumed to be fully redundant: each one allocates nominal and redundant monitoring thermistors and heating resistances. For each control stage (the four detectors FPA, M2 and M3), a thermistor reading shall be acquired and a heater adjusted every second. Mirror M1 dimensions may need a more accurate monitoring. In this case the control loop may be based on the average reading of more than one sensor, possibly up to all five allocated for M1. Only one heating line is expected for the mirror. Multiple heaters (in series or in parallel, TBD) will be energized by this single line to optimize heat distribution.

***Table 6: Preliminary list of ARIEL PLM thermistors***

| Unit | Position | Number | Type | Resolution | Accuracy |
|---|---|---|---|---|---|
| FGS | TCS | 1 (+1 Red) | Cernox | 0.025K for T ≤ 60K<br>0.1K for T > 60K | 0.050K for T ≤ 60K<br>0.25K for T > 60K |
| | DS | 1 (+1 Red) | | | |
| | Box (TBC) | 1 (+1 Red) | DT-670 | 0.25K | 0.25K |
| NIRP | TCS | 1 (+1 Red) | Cernox | 0.025K for T ≤ 60K<br>0.1K for T > 60K | 0.050K for T ≤ 60K<br>0.25K for T > 60K |
| | DS | 1 (+1 Red) | | | |
| | Box (TBC) | 1 (+1 Red) | DT-670 | 0.25K | 0.25K |
| AIRS | TCS | 1 (+1 Red) | Cernox | 5 mK for 32K< T <42K<br>0.025K for T ≤ 60K<br>0.1K for T > 60K | 0.050K for T ≤ 60K<br>0.25K for T > 60K |
| | DS | 1 (+1 Red) | Cernox | 0.025K for T ≤ 60K<br>0.1K for T > 60K | 0.050K for T ≤ 60K<br>0.25K for T > 60K |
| | Box (TBC) | 1 (+1 Red) | DT-670 | 0.25K | 0.25K |
| JT cooler | Cold end | 3 (+3 Red) | Cernox | 0.025K for T ≤ 60K<br>0.1K for T > 60K | 0.050K for T ≤ 60K<br>0.25K for T > 60K |
| I Rad | IF to detectors straps (hot spot) | 2 (+2 Red) | Cernox (TBC) | 0.025K for T ≤ 60K<br>0.1K for T > 60K | 0.050K for T ≤ 60K<br>0.25K for T > 60K |
| | Opposite positions (max grad) | 2 (+2 Red) | | | |
| OB | IF to Radiator | 1 (+1 Red) | Cernox (TBC) | 0.025K for T ≤ 60K<br>0.1K for T > 60K | 0.050K for T ≤ 60K<br>0.25K for T > 60K |
| | IF to Bipods | 3 (+3 Red) | | | |
| | Opposite positions (max grad) | 2 (+2 Red) | | | |
| | Critical optical units | 2 (+2 Red) | | | |
| Telescope | M1 | 5 (+5 Red) | Cernox (TBC) | 0.025K for T ≤ 60K<br>0.1K for T > 60K | 0.050K for T ≤ 60K<br>0.25K for T > 60K |
| | M2 + M2M | 2 (+2 Red) | DT-670 (TBC) | 0.25K | 0.25K |
| | Baffle | 3 (+3 Red) | DT-670 (TBC) | 0.25K | 0.25K |
| VG3 | Bipods IF | 3 (+3 Red) | DT-670 (TBC) | 0.25K | 0.25K |
| | Precooling/harness IF | 3 (+3 Red) | DT-670 (TBC) | 0.25K | 0.25K |
| VG2 | Bipod/harness/piping IF's | 3 (+3 Red) | DT-670 (TBC) | 0.25K | 0.25K |
| VG1 | Bipod/harness/piping IF's | 3 (+3 Red) | DT-670 (TBC) | 0.25K | 0.25K |
| *Total ARIEL PLM thermistors* | | 46 (+46 Red) | = 26 Cernox + 20 Diodes | | |

The detailed design and power requirements of the temperature control stages must rely on a realistic estimation of the possible level and time spectrum of the fluctuations on each sensitive unit or at its interfaces. The TMM can provide indications of the power (peak/max, average and power resolution) needed to be applied to the mirror(s) and detectors during operations, once the expected instabilities at the main interfaces are considered.

A preliminary evaluation of the power needs for the ARIEL PLM units has been carried out by analysis. The power allocated for detectors thermal control is 5 mW (TBC), as the SCA's are "light" units in terms of thermal capacitance. Moreover the control stage will be designed to minimize the control power by using tuned thermal resistances towards the source of instability. For the telescope control, the required power depends mainly on the final mass of the mirror(s) and on the time behavior of the fluctuations. The light-weighting level of the flight M1 will have an impact on its thermal behavior and stability. With the present thermo-mechanical design the TMM prediction for M1 max decontamination power is around 6W, with a 50% margin that includes also the fraction for M2 and M3.

In the other S/C Modes the thermal control may be limited to:

- cooldown phase during transfer to L2 (first few weeks of flight). For decontamination purposes the mirrors temperature should be kept around or above 170K (TBC) with the telescope baffle at 160K, for approximately the first two weeks of flight operations. With the present thermo-mechanical design the TMM prediction for M1, M2 and M3 max decontamination power is around 40W (with a 50% margin). This is the power needed to take M1 temperature to 170K once the mirror is already operating at 50K, in case a decontamination run is needed during cold operations. The control logic for decontamination can be based on a simple proportional loop;
- Survival/Eclipse Modes. In these operative Modes the thermal control shall be able to maintain the units temperature in their survival range (TBD). Survival heaters control can be based on a proportional control loop.

Survival/decontamination heaters control should be under S/C responsibility and will not be part of the ICU/TCU functions.

***Table 7: PLM units active thermal control required performances***

| Payload Unit | T_Op [K] | Op T range [K] | □T in time [K] | Control power [W] |
|---|---|---|---|---|
| Telescope M1 | < 70 | 50 – 70 | ± 1 | 0 – 6 |
| FGS detectors | ≤50 | 50 – 70 | ± 0.1 | 0 – 0.005 |
| NIRP detectors | ≤50 | 50 – 70 | ± 0.1 | 0 – 0.005 |
| AIRS detectors | ≤42 | 35 – 42 | ± 0.05 | 0 – 0.005 |

To date the required stability for the telescope mirror (see Table 7) is a band 2K wide (± 1K) around its operating temperature in the 50 – 70K range, in a time reference of one observation run (typically 10 hrs TBC).

For the detectors we assume that their stability level, in the time reference of one observation run (typically 10 hrs TBC), will be ±0.1K (a 200 mK wide range) around the operating T for the FGS and NIR photometer and ±0.05K (10 mK peak-to-peak) for the AIRS.

#### 2.3.5.1 Detectors temperature control stages

Detectors thermal control is achieved by the combination of passive and active damping processes. The passive component exploits the thermal inertia (R and C) of the detector system components (struts and frames) to damp temperature oscillations during their propagation from the instability source (the Instrument radiator or the JT cold end) to the detectors. The finer active control is accomplished by a PID type controller on the Thermal Control Stage (TCS). This is composed by the detector supporting flange and the active closed loop thermal control system: a heater plus thermistor couple driven by the warm electronics. Since detectors thermal stability is critical for instrument performance, a fully redundant system with two identical heater and sensor pairs is foreseen.

Each detector stage is thermally decoupled from the relative module box or optics, to ensure optimal performance in terms of absolute temperature and stability. Coupling of the detectors to the temperature reference stage (cooler cold end or radiator) is achieved through high conductance links (high purity Al straps) that connect to the TCS. The TCS works as an intermediate stage between FPA and cooling point, so it must be partially decoupled from both sides to act as a passive filter by increasing the system time

constant and to minimize the power needed for active control. The optimal conductance for the ARIEL detectors control stages has been evaluated by thermal analysis. Model results indicate that for the T control stage a conductance on the order of 0.1 W/K to the cooling stage (see Table 5) and a thermal coupling 10 times more insulating (G ~ 0.01 W/K) to the SCA's, are an acceptable compromise, in terms of control power and absolute temperature requirements. A simple schematic view of the TCS configuration is shown in Figure 9.

#### 2.3.5.2 Telescope Primary Mirror temperature control stage

The telescope M1 is supported on the optical bench by means of three structure (Figure 10). The detailed design of these struts shall to take into account the opto-mechanical requirements to ensure the telescope optical stability. The struts are made of the same alloy of the mirror (Al6061) but the thermal conductance can be controlled at the three contact points by means of thermal washers. According to the results of the present analysis, a conductance $G_{M1}$ < 0.1 W/K (TBC) is sufficient for mirror temperature control. Together with the high thermal mass of the mirror, this level of conductive decoupling from the bench allows an efficient filtering of the instabilities expected, at this stage, at higher frequencies (with periods on the order of seconds and minutes). The slower fluctuations (with periods longer than thousands of s) that could be transmitted to the optics will be smoothed by the active control system (Figure 10). This is composed by a heating line that could supply either strip heaters or film resistances (in series or parallel TBD) distributed inside the cavities of the light-weighting machining on the mirror large back surface to ensure a more even heat distribution. Control is based on a PID type feed-back loop responding to the temperature readings coming from a set of sensors located in key positions (inside the M1 back surface or on the struts) to monitor the thermal status of the mirror in all directions.

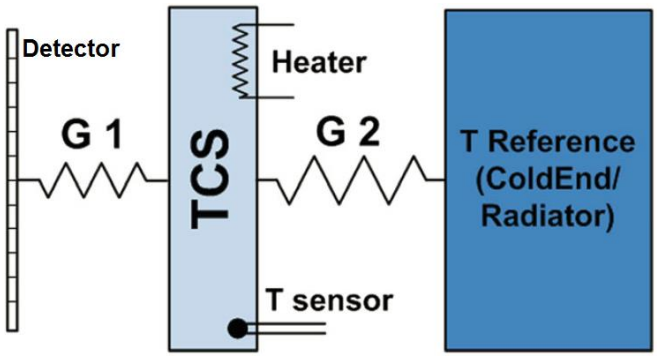


***Figure 9: Detector modules thermal control stage scheme***

### 2.3.6 Heaters

Heaters are needed for thermal control of the channels detector and telescope mirrors, plus decontamination/survival. The control heaters for the detectors could be designed to operate also for decontamination and SCA's annealing purposes (TBC), should this need arise.

For PLM thermal control film and cartridge heaters will be used. Type and resistance is still TBD at the moment. For this reason, models or resistance range has not been selected yet: thermal analysis will provide the power range and the power resolution (minimum step of power to be adjusted by TCU) needed. On this basis the heaters (type, resistance) will be selected in collaboration with ICU/TCU team. In principle all heaters are assumed to be on the 28V power line and they should be sized so that the main performance specification are satisfied even at the minimum expected voltage value from the S/C on this line during operations.

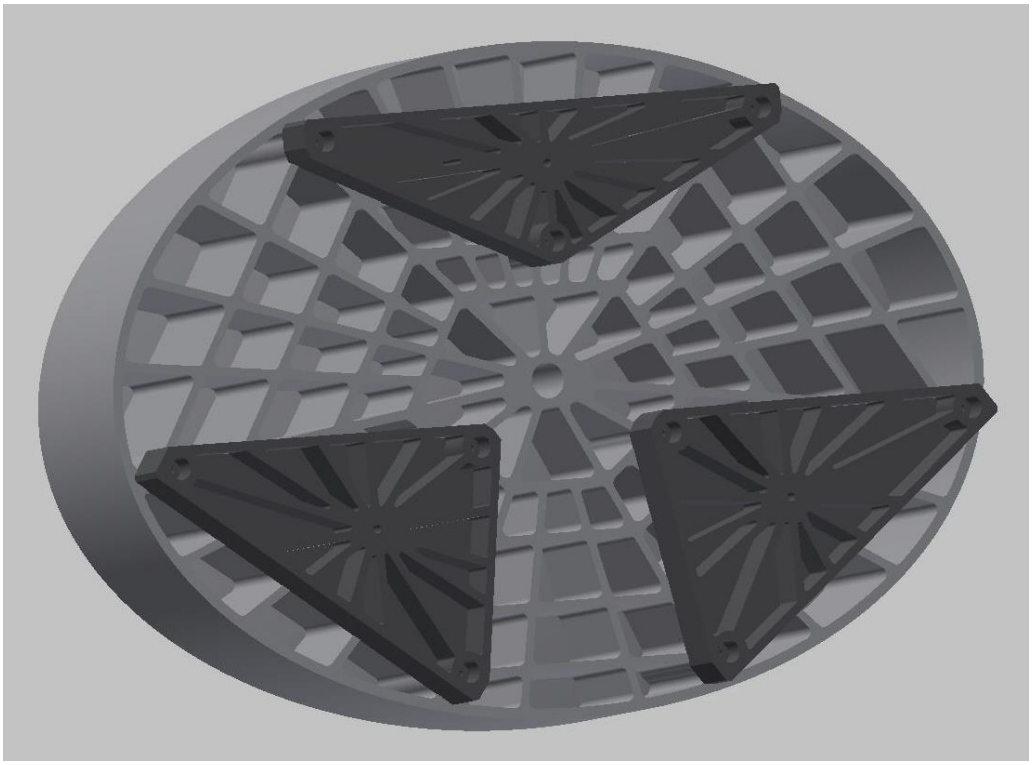

***Figure 10: Telescope M1: heaters and thermistors can be located inside the light-weighting cavities and/or on mirror supports***

At present the total number of resistors to be controlled by the ICU/TCU is 5:

- 3 nominal heaters (+3 redundant) for detectors thermal control
- 1 nominal (+ redundant) heating line for the telescope primary mirror (two if also M2 needs control)
    - each heating line can feed up to 3 to 5 resistors connected in series or parallel to distribute heat more evenly on the large mirror surface
- 1 nominal (+ redundant) heating line for the telescope decontamination/PLM survival
    - each heating line can feed several resistors connected in series or parallel

For detector control, power is expected to be in the range 0 - 2W (if detector annealing is an option), or smaller 0 - 0.1W, for each heater with a 100 uW power resolution, as the maximum power allocated for control during normal operations is 5 mW.

For telescope control the range is on the order of 0 - 6W (TBC), due to the higher thermal mass of the mirror, with a lower resolution requirement (0.1 W, TBC). The power resolution will be defined on the basis of the expected fluctuations on the mirror.

The control heaters will be operated with a PID type logic and connected to the control electronics by shielded twisted pairs to minimize EMI. The number of heating lines (as some of them could energize more than one resistor) are summarized in the following table.

***Table 8: Preliminary list of ARIEL control heaters***

| Unit | Position | Number | Type | Resistance Ω) | Range (W) | Resolution (mW) |
|---|---|---|---|---|---|---|
| FGS | TCS | 1 (+1 Red) | Cartridge/Film | TBD | 0 – 0.1<br>0 – 2 | 0.1 (TBC) in 0-100 mW range<br>100 in the 0 - 2W range |
| NIRP | TCS | 1 (+1 Red) | Cartridge/Film | TBD | 0 – 0.1<br>0 – 2 | 0.1 (TBC) in 0-100 mW range<br>100 in the 0 - 2W range |

| | | | | | | |
|---|---|---|---|---|---|---|
| AIRS | TCS | 1 (+1 Red) | Cartridge/Film | TBD | 0 – 0.1<br>0 – 2 | 0.1 (TBC) in 0-100 mW range<br>100 in the 0 - 2W range |
| Telescope | M1 | 1 (+1 Red) | Cartridge/Film | TBD | 0 - 10 | 100 (TBC) in the full range |
| Decon/survival | PLM units | 1 (+1 Red) | Cartridge/Film | TBD | 0 – 40 (TBC) | TBD |
| *Total PLM heaters* | | 5 (+5 Red) | | | | |

### 2.3.7 Harness preliminary thermal analysis

Detectors wiring plus all the service harness (general HK, thermal control, heaters, thermistors etc.) consists of a high number of electrical connections. An appropriate selection of materials combined with an optimal combination of gauge wiring and harness length allows to keep the conducted load from the warm SVM to the coldest stages within few tens of mW. In order to minimize parasitic loads to TOB, radiator and cooler cold end, all the passive stages should be used for heat leak interception. In particular, the last V-Groove (VG3) is the main and final harness thermalization stage to minimize the load of the FEE on the detectors. At the same time, working as a conductive link, the warm harness can also be used to efficiently remove cold electronics heat load towards the VG3, if needed.

A preliminary estimation of the possible heat loads due to instrument wiring on the stages, has been carried out on the basis of conservative assumptions (ref. [RD02]). The results, in terms of heat leaks to the thermal stages, are summarized in Table 9.

***Table 9: Heat loads due to harness***

| Harness | VG1 (TIF1) [mW] | VG2 (TIF2) [mW] | VG3 (TIF3) [mW] | TOB (TIF5) [mW] | JT cold end (TIF6) [mW] |
|---|---|---|---|---|---|
| Detectors control[1] | 182 | 101 | 64 | 8.0 | TBD |
| Thermal control[2] | 64 | 35 | 22 | 2.7 | 0.8 |
| M2 control | 10 | 5 | 3 | 0.4 | - |
| Calibration source | 10 | 5 | 3 | 0.4 | - |
| Total load | 266 | 147 | 93 | 11.5 | 0.8 |
| **Total load w/ 50% margin** | 399 | 220 | 140 | 17 | 1.3 |

The contribution of the AIRS cryo harness connecting the CFEE's to the SCA's (around 1 mW) is, at this stage, considered part of the detector system budget and is already included in the active load estimation of the two FPA's (Table 3) assumed for the thermal analysis.

In the next advanced phase of the PLM design, a detailed analysis will allow to trade thermal performance with the electrical properties, reliability, mass and complexity for harness design optimization.

# 3 PLM GMM AND TMM

## 3.1 MATERIAL PROPERTIES

A summary of the values of material properties assumed in the model are shown in this chapter.

### 3.1.1 Bulk material properties

For the thermal analysis purpose, the density, the specific heat and thermal conductivity are the bulk properties defined and used. The specific heat and the conductivity are defined as temperature dependent functions over the whole range covered by the analysis. The bulk material used are:

- Al 6061
- Aluminium Honeycomb
- Glass Fibre Reinforced Polymer (GFRP)
- GFRP internal foam

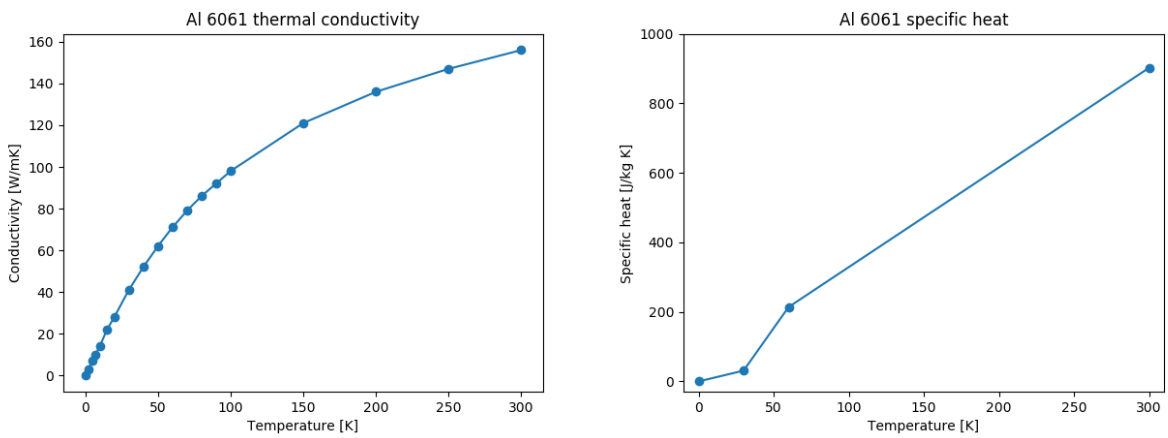


***Figure 11: Al 6061 thermal conductivity and specific heat with respect to temperature.***

The Al 6061 has a density of 2707 kg/m$^3$, Figure 11 shows the values used for the thermal conductivity and the specific heat as a function of temperature.

The Aluminium Honeycomb property is assigned to the geometries representing the honeycomb core of a sandwich panel. Honeycomb is an orthotropic material, the conductivity differs along the in-plane and cross-sectional directions. Two effective conductivities for the honeycomb are calculated using the two following formulas:

$$k_{in-plane} = 1.25\frac{\delta}{S}k_{Al\ 6061}$$

$$k_{through\ thickness} = \frac{8}{3}\frac{\delta}{S}k_{Al\ 6061}$$

Where $\delta$ is the nominal foil thickness, S is the cell size. The formulas, taken from Spacecraft Thermal Control Handbook, Gilmore D., are valid for hexagonal cell structures. The present assumptions on the honeycomb configuration have been derived for the indications of the ESA CDF study: $\delta$ =0.0007 inches and S= 3/16 inches, giving a $\delta$/S ratio equal to 3.73 x 10$^{-3}$, corresponding to a density close to 32 kg/m$^3$. The in-plane and through thickness conductivities for the honeycomb are also vector quantities, functions of the temperature since they are calculated from the Al 6061 conductivity.

The GFRP has a density of 1948 kg/m$^3$, Figure 12 shows the values used for the thermal conductivity and the specific heat vs temperature.

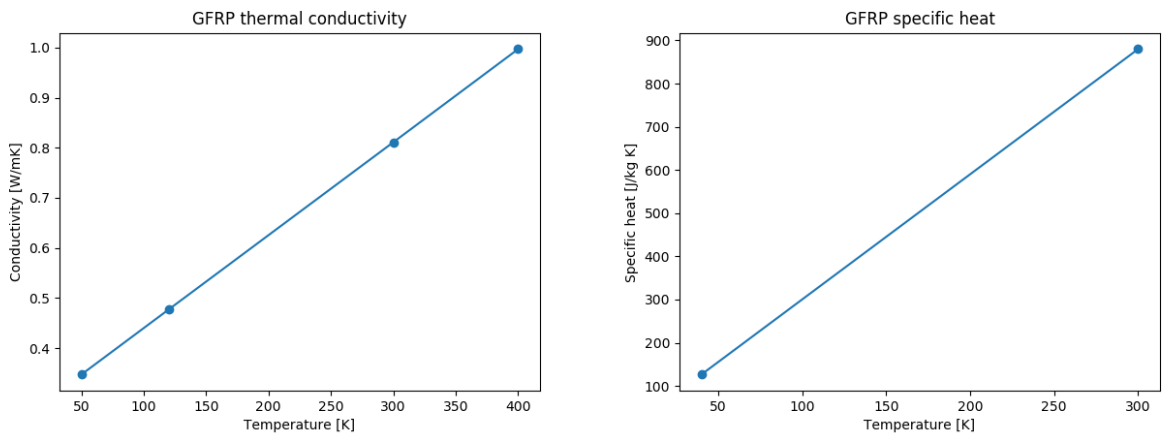


***Figure 12: GFRP thermal conductivity and specific heat with respect to temperature.***

The bipod legs are filled with a stiffening foam to increase rigidity. The bulk properties for this material have been assumed on the basis of previous missions like Planck, plus a large extra margin to include uncertainties: density of 1900 kg/m$^3$, nearly one tenth of the GFRP conductivity (worst case), and the same specific heat of the GFRP (worst case).

### 3.1.2 Thermo-Optical properties

Thermo-Optical properties are assigned to the geometrical model surfaces to characterise their radiative thermal behaviour. The values of emissivity $\varepsilon$, absorptivity $\alpha$, diffusive and specular reflection $\rho$ in the infrared and solar bands for the thermo-optical properties used in the GMM are shown in Table 10.

***Table 10: Thermo-optical properties used in ESATAN-TMS***

| | *Infrared band* | | | *Solar band* | | |
|---|---|---|---|---|---|---|
| | $\varepsilon$ | $\rho_{DIFFUSIVE}$ | $\rho_{SPECULAR}$ | $\alpha$ | $\rho_{DIFFUSIVE}$ | $\rho_{SPECULAR}$ |
| Black Paint | 0.90 | 0.10 | 0.00 | 0.94 | 0.06 | 0.00 |
| VDA | 0.05 | 0.90 | 0.05 | 0.13 | 0.85 | 0.02 |
| Silver (Mirrors) | 0.02 | 0.03 | 0.95 | 0.04 | 0.01 | 0.95 |
| MLI (SVM boundary) | 0.05 | 0.95 | 0.00 | 0.12 | 0.88 | 0.00 |

## 3.2 DESCRIPTION OF THE GEOMETRICAL MATHEMATICAL MODEL (GMM)

The GMM is based on the CAD model of the PLM. Small geometries and details which are not relevant for thermal analysis purposes are not considered in the GMM. In the model the main radiative surfaces and representative supporting structures between the different stages are simulated.

### 3.2.1 SVM/PLM Interface

In order to simulate the interaction with the Service Module, the model includes the SVM/PLM interface assumed as a boundary. The SVM/PLM I/F is composed by two surfaces with the dimensions indicated in Figure 4). The conductive one is called “SVM top plate”, operates at room temperature and is the main interface of the bipods and V-Grooves struts. The other surface is the “SVM Radiative shield”, located in between the SVM top plate and the VG1, and represents a purely radiative coupling with the rest of the model. The SVM top plate is a disc of diameter 2700 mm, cut to 2400 mm in the $\pm Y_{ARIEL}$ axis. Figure 13 shows front views of the entire model in ESATAN-TMS. The SVM top plate is colored in orange, the SVM

Radiative shield in yellow. These two shells have assigned optical coating MLI which has a low value of emissivity (0.05).

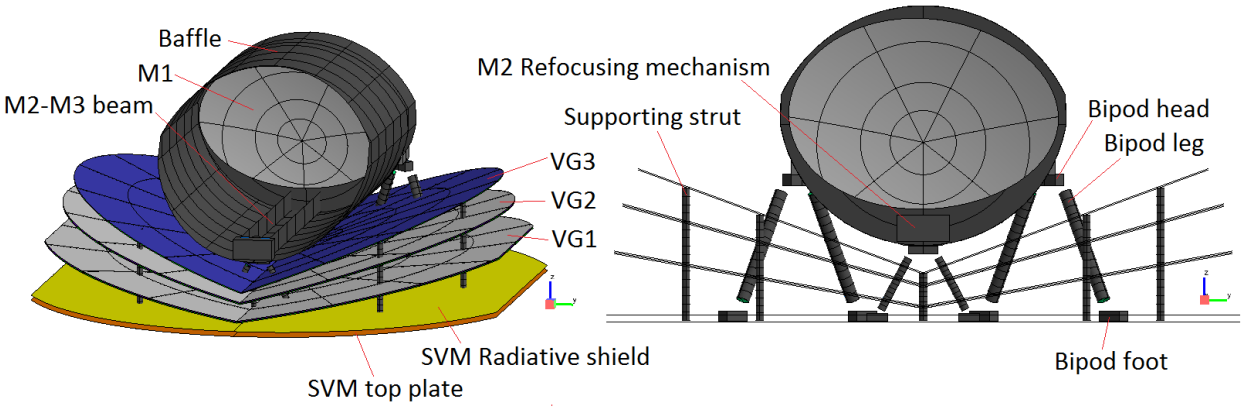


***Figure 13: Front views of the PLM GMM with the SVM/PLM I/F.***

### 3.2.2 V-Grooves

The PLM first cooling stage is represented by the V-Grooves (VGs), which are designed as three couples of semi-circular panels with an inclination set of 10°-15°-20°. The VGs are sandwich panels with Aluminium alloy hexagonal honeycomb core and Al 6061 external surfaces. All surfaces of the VGs are coated with VDA (Vapour Deposited Aluminium, emissivity ~0.045) with the exception of the upper surface of the topmost VG which is covered by an open aluminium honeycomb coated with black paint to maximise the heat exchange with the cold space.

The entire PLM passive cooling works only if the spacecraft cold section is shaded from the Sun once in orbit. The maximum allowed Solar Aspect Angle (SAA), with respect to the nominal attitude (Sun vector perpendicular to the SVM platform) is ±30° along the $\pm Y_{ARIEL}$ axis and ±6° along the $\pm X_{ARIEL}$ axis. This requirement, together with the dimensions of the SVM/PLM I/F, poses a limit on the maximum dimensions of the VGs. The radii of the designed VG's are 1260, 1180, 1150 mm, respectively from the lowest to topmost. In order to have all three VGs inside the allowed envelope, it is necessary to cut the lowest VG (VG1) at the $\pm Y_{ARIEL}$ ends with a plane inclined of 6° from the SVM top plate. The other two VGs (central and topmost) fit already inside the shadowed envelope.

The VGs sandwich panels are modelled in detail in ESATAN-TMS in order to consider the different thermal properties of the external skins and the honeycomb core. Each VG semi-circle is composed of three identical shell geometries, representing the two skins and the honeycomb. Two different conductivities are defined to model the in-plane and the though thickness transverse heat flows (see paragraph 3.1.1).

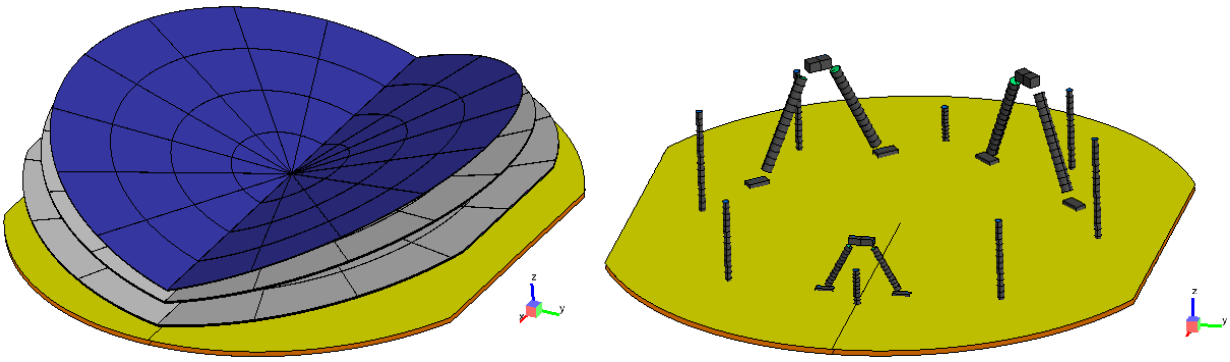

***Figure 14: The three V-Grooves (left panel) and bipods plus supporting struts (right panel) connecting the SVM to upper and coldest parts of the PLM.***

### 3.2.3 Bipods and supporting struts

Three bipods and eight supporting struts connect the VG's, the OB and the telescope structure to the SVM top platform (Figure 14, right). The bipods support the telescope structure and the Optical Bench (TOB). The struts are needed to support the V-Groove petals.

Pod legs and supporting struts are made of GFRP and are modelled with hollow cylinder geometries. The bipods feet and heads are sketched as Al 6061 boxes, thermally linked to the legs with a calculated conductance. This value is calculated assuming Al alloy fixtures instead of Ti6Al4V (which is the current design baseline): the results is that each fixture between the leg and the foot, in the TMM, has a conductance overestimated by a factor more than 20. This is obviously a worst case assumption for the evaluation of the bipod legs total conductance. The legs are filled with a special rigid foam to enhance their structural properties. The foam contribution is taken in account in the thermal model by assigning a conductivity only slightly lower than GFRP (by 10%) and considering the foam as a dense material. This is an obvious worst case in the evaluation of the through and contact conductance. The characteristics of the bipods and struts are summarized in Table 11. Dedicated links (user defined conductors) are evaluated to model the straps that thermally connect them to the V-Grooves.

***Table 11: Bipods and supporting struts characteristics***

| Structure | Diameter | Thickness |
|---|---|---|
| Front bipod (M2 side) | 30 mm | 3.0 mm |
| Internal foam inside front bipod legs | 28 mm | 28 mm |
| Rear bipods (M1 side), x2 | 50 mm | 5.0 mm |
| Internal foam inside rear bipod legs | 48 mm | 48 mm |
| Supporting struts, x8 | 30 mm | 1.5 mm |

### 3.2.4 Telescope, Baffle and Telescope Optical Bench

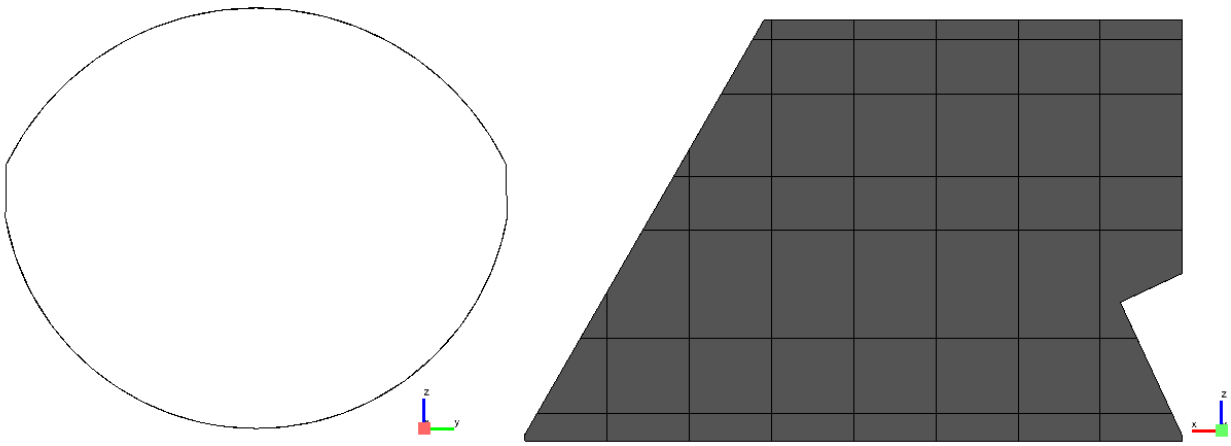

***Figure 15: Front and lateral views of the Baffle.***

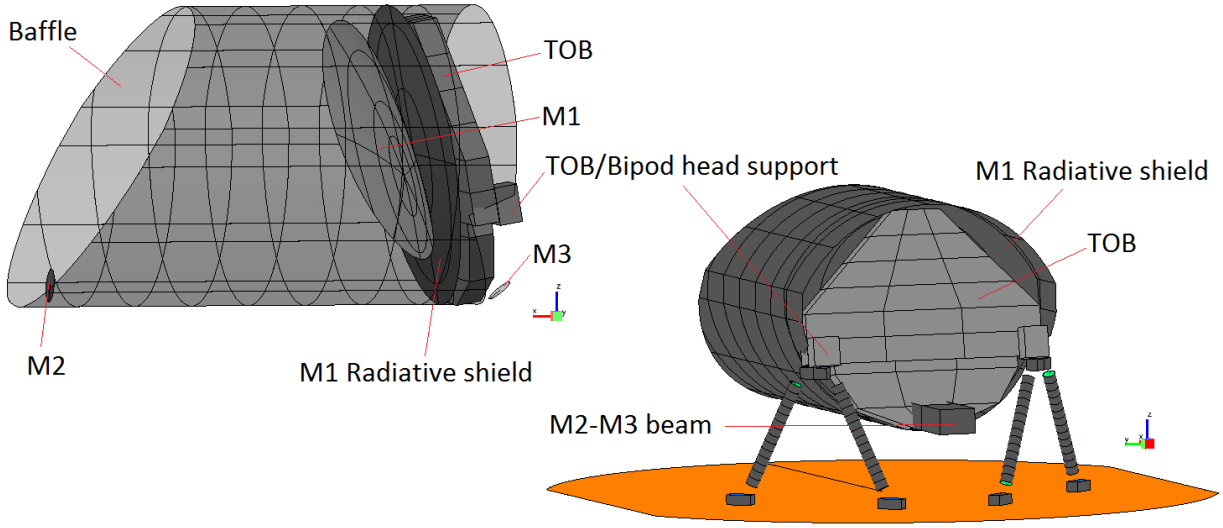


***Figure 16: Side view (up-left) and rear view (down-right) of the Baffle, Telescope, TOB assembly. In the side view, the Baffle geometries are transparent to let see internal components.***

In the G/TMM the telescope assembly is considered composed by the structure (beam), the baffle, the OB and the M1, M2 and M3 mirrors. The M1 mirror (1100 mm x 750 mm) is simulated by a cut paraboloid shape while M2 and M3 are simple disc shells. The bulk material of the mirrors is Al 6061 and their thermo-optical property is a very low emissivity surface, 0.02 (Silver), while the back is assumed black painted. The M1 thickness is 200 mm but the mirror is not a full bulk of Al 6061. In order to take into account the light-weighting cavities of the M1 back structure, an effective thickness of 50 mm is applied to the M1 shell geometry to replicate a total mass of ~90 kg.

The baffle structure is a composition of two circular cut cylindrical shells of different radius vertically connected at their edges with two smaller rectangular surfaces (Figure 15). The whole baffle structure has a front cut at 30° with respect to the $YZ_{ARIEL}$ plane, and another cut at rear-bottom to allow insertion of the bipods' interface with the TOB (Figure 16). The baffle external surface has an open honeycomb configuration, as the VG3. In order to model the in-plane and through-plane conductivity, the shells are assumed as Al 6061 surfaces with an effective thickness which takes into account the conductance of the Aluminium skin and the honeycomb composite structure. The external and internal surfaces of the baffle are black painted in order to have a high efficient radiative exchange to cold environment and to minimize stay-light reflections in the inner volume of the telescope.

The M2 is placed at the front aperture of the Baffle. Behind it, the M2 refocus mechanism is simply designed as a box. The M2 with its refocusing mechanism is connected to the OB by the telescope beam, that extends through the TOB. The beam is composed of three rectangular shells forming the shape of a "U" (like a box without the top side). The beam is also Al 6061, black painted.

The TOB shape and dimensions are based on the CAD design and it is sketched as a box composed by a series of trapezoidal and rectangular shell geometries. The TOB is not in a vertical position wrt to the $YZ_{ARIEL}$ plane but inclined by 10° and located at the rear side of the Baffle. Each shell composing the TOB is Al 6061, 5 mm thick and coated with black paint.

It can be noticed that the TOB does not fit perfectly in the Baffle rear aperture, leaving the edges of the M1 rear side in view of the environment. In order to protect the M1 back surface from thermal loads and induced gradients coming from the TOB and to shield the telescope internal volume from unwanted straylight, a radiative shroud is placed between the M1 and the TOB. The M1 radiative shroud is a simple shell geometry (a black coated Kapton/Al film thermally connected to the baffle), parallel to the TOB, matching the contour of the Baffle. In this way, the M1 and the baffle internal volume are radiatively decoupled from the TOB and from the environment.

### 3.2.5 Instrument assembly

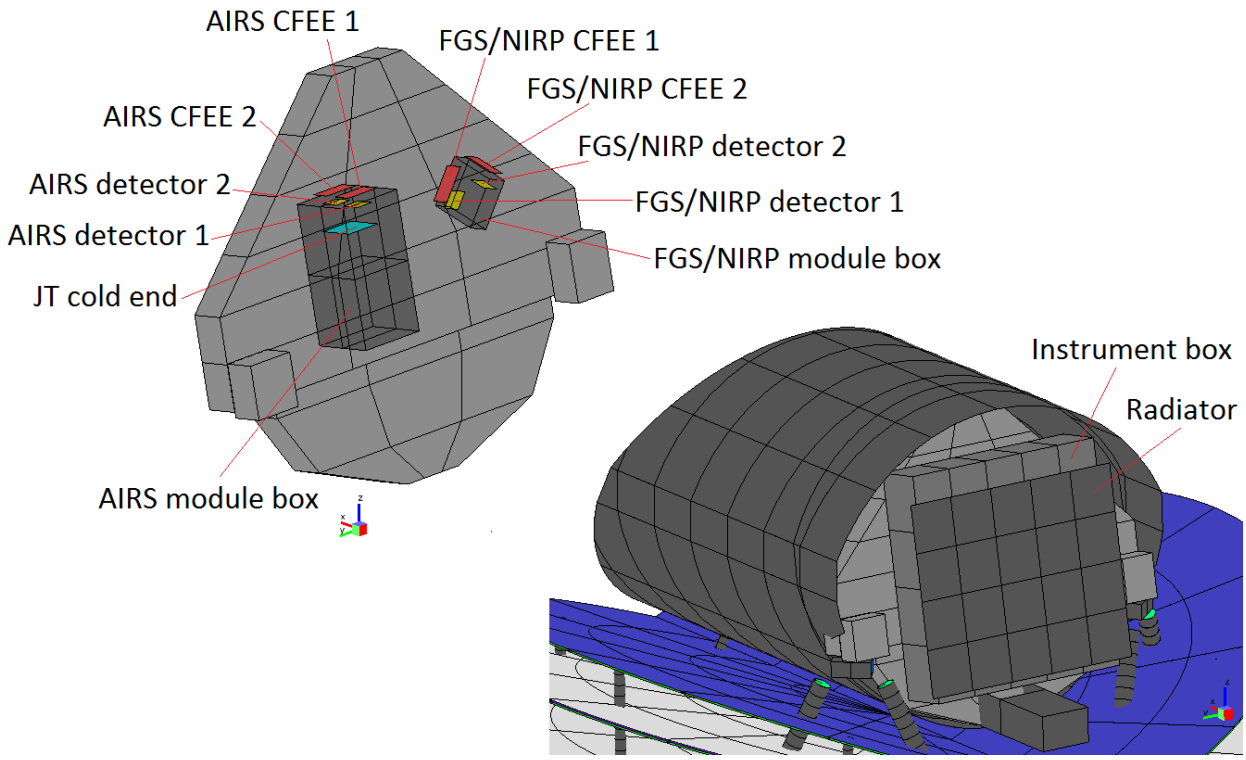


***Figure 17: The upper left panel is a detailed view, through transparent module boxes, of the components inside the Instrument box. The CFEE are coloured in red, the detectors in yellow, the JT cold end in cyan. In the bottom-right panel a rear view of the PLM, with all geometries visible, is shown.***

On the back of the telescope assembly, the TOB accommodates the instrument box that includes the two channel modules, FGS and AIRS, with the Cold Front End Electronics (CFEE) located on the external wall of each box adjacent to the detectors position. Each instrument is modelled as an Al 6061 box, black painted, containing the detectors. The AIRS module box contains also the active JT cooler cold end interface which is conductively linked to the two AIRS detectors.

A radiator (Instrument Radiator) of rectangular shape is located above the OB box that include the modules. The function of the instrument radiator is to provide a temperature cold reference for the FGS/NIRP detectors. It thermo-optical configuration is the same black painted open honeycomb structure of the Baffle.

The thermal model components and related properties are reported in the Table below.

***Table 12: GMM nodes properties***

| Main components | Node # | Bulk Material | Optical Coating |
|---|---|---|---|
| Bipods (foot, heads, legs) | 1-273 | GFRP | Black Paint |
| Bipod internal foam | 300-899 | GFRP modified | -- |
| Radiative shield M1 - TOB | 1200-1211 | Al6061 | Black Paint |
| Instrument Box | 1600-1657 | Al 6061 | Black Paint |
| AIRS Box | 2000-2015 | Al 6061 | Black Paint |
| AIRS CFEE 1 | 2100 | Al 6061 | Black Paint |
| AIRS CFEE 2 | 2110 | Al 6061 | Black Paint |
| AIRS detector 1 | 2200 | Al 6061 | -- |

| | | | |
|---|---|---|---|
| AIRS detector 2 | 2210 | Al 6061 | -- |
| AIRS TCS detector 1 | 2300 | Al 6061 | -- |
| AIRS TCS detector 1 | 2310 | Al 6061 | -- |
| JT Cold End | 2500 | Al 6061 | -- |
| FGS/NIRP Box | 2600-2605 | Al 6061 | Black Paint |
| FGS/NIRP CFEE 1 | 2700 | Al 6061 | Black Paint |
| FGS/NIRP CFEE 2 | 2710 | Al 6061 | Black Paint |
| FGS/NIRP detector 1 | 2800 | Al 6061 | -- |
| FGS/NIRP detector 2 | 2810 | Al 6061 | -- |
| FGS/NIRP TCS detector 1 | 2900 | Al 6061 | -- |
| FGS/NIRP TCS detector 2 | 2910 | Al 6061 | -- |
| Mirror 1 (M1) | 3000-3126 | Al 6061 | Silver / Black Paint |
| Mirror 2 (M2) | 3200 | Al 6061 | Silver / Black Paint |
| Mirror 3 (M3) | 3202 | Al 6061 | Silver / Black Paint |
| Telescope Optical Bench (TOB) | 3000-5305 | Al 6061 | Black Paint |
| V-Groove1 | 10000-11131 | Honeycomb/Al 6061 | VDA |
| V-Groove2 | 11200-12331 | Honeycomb/Al 6061 | VDA |
| V-Groove3 | 12400-13131 | Honeycomb/Al 6061 | VDA / Black Paint |
| Telescope Baffle | 13200-13741 | Al 6061 | Black Paint |
| Supporting struts | 14000-15413 | GFRP | Black Paint |
| Instrument Radiator | 17000-17019 | Al 6061 | Black Paint |
| M2 Refocusing Mechanism | 17200-17205 | Al 6061 | Black Paint |
| Beam Telescope | 17300-17452 | Al 6061 | Black Paint |
| SVM top plate | 20000 | Al 6061 | MLI |
| SVM Radiative shield | 21000 | Al 6061 | MLI |

The detectors of both AIRS and FGS/NIRP and the JT cold end geometries have no optical properties assigned at the moment. Their thermal radiative coupling is considered negligible at this stage and will be more accurately modeled in the next issue of the model.

### 3.2.6 Radiative cases

In this chapter, that closes the description of the ARIEL PLM geometrical model, are reported the radiative cases that have been run on the GMM. The radiative cases define how the model interacts with the environment. Two main scenarios have been taken into account for the analysis of the ARIEL PLM:

1. GMM during the routine orbit around the Earth-Sun L2 point
2. GMM during Low Earth Orbit Phase (LEOP)

In the first scenario, the PLM is placed at a circular Sun-centered orbit at 1.5 x $10^6$ km from the Sun, with the SVM plate perpendicular to the Sun vector. The Sun illuminates the lower surface of the SVM top plate which totally shields the PLM from solar radiation. As described in the next section, in the present model assumptions the SVM top plate is simulated as a boundary node with a fixed temperature condition. Given the assumed radiative configuration, the PLM always results fully shaded from the Sun as far as the S/C attitude rotation remains within the allowed SAA (±6° $X_{ARIEL,}$ ±30° $Y_{ARIEL}$). For this reason no radiative case

with varying SAA has been computed. Case 1 is the radiative reference for the nominal orbit steady-state Hot and Cold TMM cases and is also used for the cooldown, decontamination and SVM T variation transient analyses.

Case 2 is used to study the exposure of the cold PLM to the solar radiation during launch and early operations. The Mission Analysis Guidelines (MAG) document [AD4] describes the baseline scenario for LEOP operations and indicates the assumptions that must be considered on the possible orientations of the Sun vector relative to the PLM. These orientations are summarized in Figure 18: the Sun vector is allowed everywhere except for the volume defined by the two red cones. The cones have an aperture of ±65° around the $\pm X_{ARIEL}$ so the Sun may be in an angle range between 65-115° from the $\pm X_{ARIEL}$ axis (or ±25° from the $\pm Z_{ARIEL}$ axis). In order to carefully analyse the possible impact on the PLM of this scenario, a different set of Sun vectors have been considered, each one corresponding to a single radiative case. Only Sun vectors in the $+Z_{ARIEL}$ hemisphere have been studied, where the cold PLM is exposed to the solar radiation, as this is the off nominal and worst case configuration.

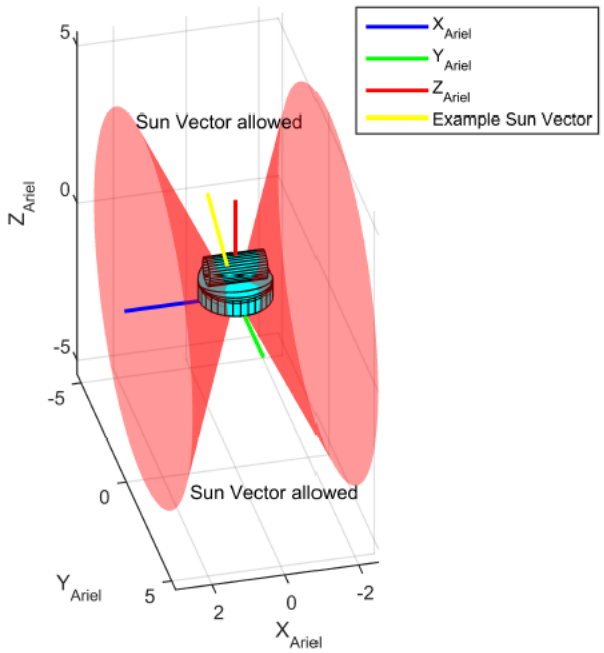


*Sun vectors considered:*

- In the $XZ_{ARIEL}$ plane, from the $+X_{ARIEL}$ axis
  - a) 65° (tangent to the $+X_{ARIEL}$ red cone)
  - b) 90° (equal to the $+Z_{ARIEL}$ axis)
  - c) 95°
  - d) 100°
  - e) 115°(tangent to the $-X_{ARIEL}$ red cone)
- In the $YZ_{ARIEL}$ plane, from the $+Y_{ARIEL}$ axis
  - f) 65°
  - g) 80°

***Figure 18: Sun vector allowed zone during ascent phase. The Sun vector is allowed outside the two red cones. Figure taken from MAG document.***

For each Sun vector, the relative radiative case has been run and then the steady-state solution has been computed with the TMM, in order to identify the direction which causes the worst illuminating conditions for the PLM. Once this worst case has been identified, then it was used for the main transient analysis. The results of the full analysis (radiative and conductive) are reported in Chapter 4.

## 3.3 DESCRIPTION OF THE THERMAL MATHEMATICAL MODEL (TMM)

### 3.3.1 Conductive interfaces between geometries

All the options allowed by ESATAN-TMS Workbench are used to define conductive interfaces:

1. Auto-generated conductive interfaces between shell geometries
2. Contact zones
3. User-defined conductors

Auto-generated conductive interfaces are used to couple the central nodes of the two semi-circle geometry of each VG, the edges of the geometries composing the Baffle, and the TOB, the side edges of all the boxes sketched. Figure 19 shows a front and a rear view of the model with the auto-generated conductive interfaces in yellow.

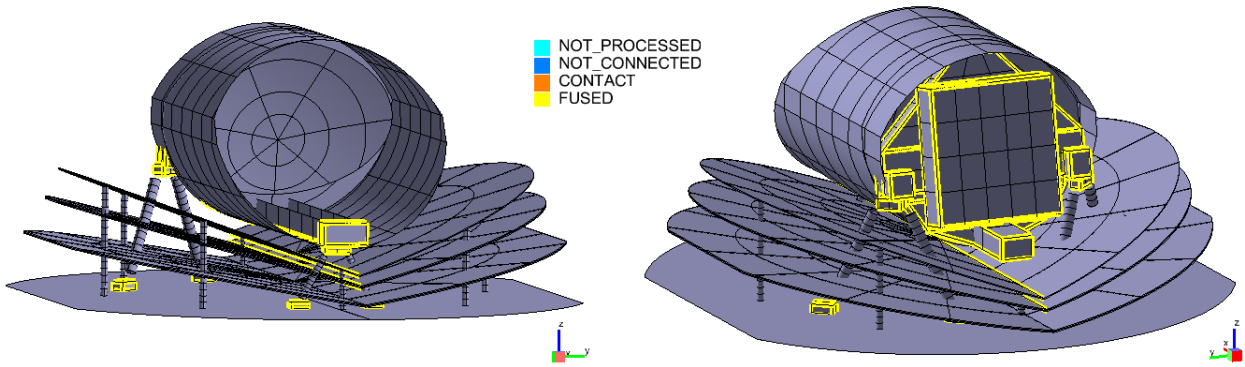


***Figure 19: Auto-generated conductive interfaces in the model (the SVM Radiative shield and the Instrument Radiator are hidden for clarity).***

Figure 20 shows the auto-generated conductive interfaces for the Baffle and VG1 calculated before the shell cuts. Only the conductors that do not reference to cut nodes, are then saved to be included in the TMM solutions.

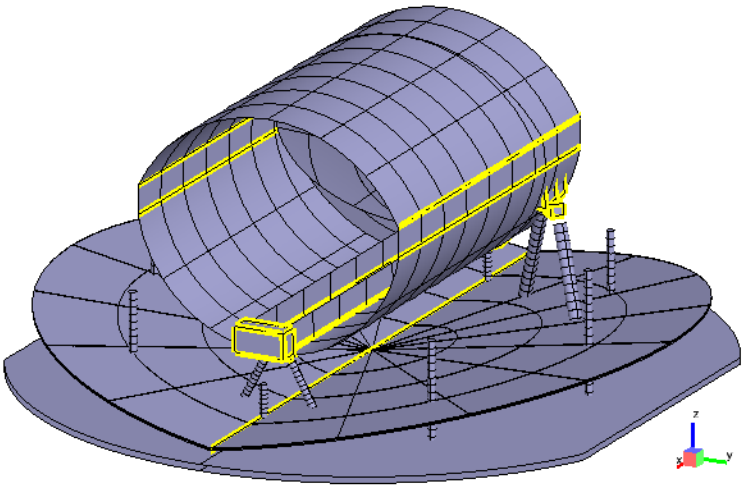

***Figure 20: The copy of the original model without the cuts on the Baffle and VG1 for the auto generation of conductive interfaces (VG2 and VG3 are hidden for clarity).***

Contact zones and user-defined conductors are used to manually add GL conductors between nodes of different geometries not involved in the auto-generated conductive interfaces. Table 13 reports the characteristics of the contact zones defined in the model.

***Table 13: Characteristics of the contact zones defined in the model.***

| Involved geometries | Total contact area [m$^2$] | Contact conductance [W/m$^2$K] | Description / Comments |
|---|---|---|---|
| SVM top plate – Bipods' feet | 0.0024 (front bipod, each foot)<br>0.005 (rear bipods, each foot) | 800 | The feet of the bipods are mechanically linked to the SVM top plate. Each bipod has two feet. The two rear bipods are identical, the front bipod is smaller. |
| Front bipod head – Baffle | 0.00339 | 100 | In the TMM it is assumed that the baffle is thermally linked to the front bipod head |
| Bipods' legs – Internal foam | 0.01935<br>(front bipod legs)<br>0.06786<br>(rear bipod legs) | 100 | Contact conductance of the rigid foam with the inner wall of the bipod leg (worst case) |
| VG skin – VG honeycomb | 2.453 (VG1)<br>2.184 (VG2)<br>2.073 (VG3) | 1000 | VG1 and VG2 are sandwich panel (two external skins and the core honeycomb), while the VG3 is open honeycomb, with no |

| | | | |
|---|---|---|---|
| | | | upper skin. |
| M2 Mechanism box - Baffle | 0.015 | 100 | The box representing the M2 refocusing mechanism is connected to the beam |
| M2-M3 Beam - Baffle | 0.02375 | 100 | The bottom side of the M2-M3 Beam in the TMM is assumed in contact with the Baffle. |
| TOB – Instrument box | 0.37573 | 1000 | The TOB and the Instrument box are a single system, for this reason a high contact conductance is considered. |
| AIRS module box – Instrument box | 0.054 | 100 | The AIRS module box bottom plate is connected to the Bench / Instrument box |
| FGS/NIRP module box – Instrument box | 0.0121 | 100 | The FGS/NIRP module box bottom plate is connected to the Bench / Instrument box. |

User-defined conductor are used to create a single node-to-node conductive link. Table 14 reports the characteristics of the user-defined conductors in the model.

***Table 14: Characteristics of the user-defined conductors used in the model.***

| Involved nodes | Conductance [W/K] | Comments |
|---|---|---|
| SVM top plate – Lowest node of each supporting struts | 0.1 each | Supporting struts are mechanically attached to the SVM top plate. |
| Foot of each bipod (top side node) – lowest node of the corresponding leg | 0.6 each | Calculated as kA/l, where k is the conductivity of Al 6061 at 280K (150 W/m-K), A is the cross-sectional area of the junction (8 x $10^{-5}$ $m^2$), l is the length of the junction (0.02 m). This assumption is a worst case as the fixture between foot and leg is made of Ti alloy |
| Head of each bipod (bottom side node) – Highest node of the corresponding leg | 0.26 each | Calculated as kA/l, where k is the conductivity of Al 6061 at 53K (65 W/m-K), A is the cross-sectional area of the junction (8 x $10^{-5}$ $m^2$), l is the length of the junction (0.02 m). This assumption is a worst case as the fixture between foot and leg is made of Ti alloy |
| VGs – Bipods' legs (each leg for each VG) | 0.1 each | The legs of the bipods are linked to the VGs in order to intercept heat leaks from the SVM. One (or two) 5N Al straps |
| VGs – Supporting struts (each strut for each VG) | 0.001 each | VGs are also supported by the struts but with insulating mountings |
| M2 – M2 Mechanism (closest node to M2) | 0.1 each | Support to M2 |
| M3 – M2-M3 Beam (closest node to M3) | 0.1 each | Support to M3 |
| Heads of the rear bipods (top side nodes) – TOB (bottom side node of the interface with the bipods) | 357.5 each | Calculated as kA/l, where k is the conductivity of Al 6061 at 53K (65 W/m-K), A is the cross-sectional area of the junction (5.5 x $10^{-3}$ $m^2$), l is the length of the junction (0.001 m). |
| TOB – Baffle (between facing node in the 3 locations) | 0.2 each | TOB is connected to the Baffle in 3 spots: at the top of the TOB, at the right and left end sides of the TOB. |
| Telescope Assembly stiffening arms: TOB – M2 refocusing box (2 node pairs, at the two central lateral sides of the TOB, and the two lateral sides of the M2 box) | 0.036 each | Two stiffening arms with hollow cylindrical shape of Al 6061 run from each lateral side of the TOB, passing under the lower sides of the Baffle, and connect to the mechanical structure of the M2. At the moment the thermal effects of these two supports is simulated with two conductive links between the TOB and the M2 box. Each strut have external and internal diameter of 50 mm and 40 mm respectively. The length is 1200 mm. The link is then calculated as kA/l, where k is the conductivity of Al 6061 at 49K (60.8 W/m-K), A is the cross-sectional (7.1 x $10^{-4}$ $m^2$), l is the length. In the next issue of the model the two struts will be simulated by cylindrical shells, black painted to optimize heat rejection to space. |
| M1 –TOB (3 node pairs) | 0.1 each | M1 is considered connected to the TOB by 3 supports (see Figure 21). These connectors simulate the three triangular shaped whiffletree mountings of M1 on the |

| | | |
|---|---|---|
| | | OB |
| FGS/NIRP detector 1 – TOB<br>FGS/NIRP detector 2 – TOB | 0.01 each | Mechanical supports of the FGS/NIRP detector on the box |
| AIRS detector 1 – TOB<br>AIRS detector 2 – TOB | 0.0005 each | Each detector is supported by 6 pods of Ti-alloy (~3.0 W/m-K conductivity at 40K). Each pod is 0.15 mm thick and has an external diameter of 2.8 mm (1.25 x $10^{-6}$ $m^2$ cross-sectional area) and is 42 mm length. |
| FGS detector 1 – FGS CFEE 1<br>FGS detector 2 – FGS CFEE 2 | 0.01 each | Cryo harness. Conductance estimated on the basis of "standard" baseline SCA's flexi cables (Cu, TBC) |
| AIRS detector 1 – AIRS CFEE 1<br>AIRS detector 2 – AIRS CFEE 2 | 0.0001 each | Cryo harness. Conductance assumed after thermal optimization of the flexi cable: wire materials is Constantan (Euclid project study heritage) see AIRS module documentation [RD4] |
| FGS CFEE 1 – FGS module box<br>FGS CFEE 2 – FGS module box | 0.01 each | Mechanical support between CFEE and module box. Insulating washers to decrease surface contact conductance by a factor of 5 |
| AIRS CFEE 1 – AIRS module box<br>AIRS CFEE 2 – AIRS module box | 0.01 each | Mechanical support between CFEE and module box. Insulating washers to decrease surface contact conductance by a factor of 5 |
| FGS CFEE 1 – TOB (closest node)<br>FGS CFEE 2 – TOB (closest node) | 0.2 each | Detectors control and HK harness from OB to CFEE |
| AIRS CFEE 1 – TOB (closest node)<br>AIRS CFEE 2 – TOB (closest node) | 0.2 each | Detectors control and HK harness from OB to CFEE |
| FGS detector 1 – Radiator (closest node)<br>FGS detector 2 – Radiator (closest node) | 0.1 each | The Instrument radiator is the cold reference for the two FGS/NIRP detectors. At present it is assumed that the detectors can be connected to the radiator node closest to their position. |
| AIRS detector 1 – JT cold end<br>AIRS detector 2 – JT cold end | 0.1 each | The JT cold end is the cold reference for the two AIRS detectors. At present it is assumed that the cold tip can be located in proximity (within 0.2 m) |
| Instrument box – Radiator (4 links, each at one of the 4 corners) | 0.01 each | The instrument radiator is attached above the instrument box by insulating connections on each of the four corners to partially decouple the radiating surface from any possible instability in the OB. |
| SVM top plate – VG1<br>VG1 – VG2<br>VG2 – VG3<br>VG3 – TOB | 0.002 each node pair, for each line | Electric harness from the SVM to the TOB passing through the VGs for heat leaks interception. In order to have a symmetrical distribution of heat, two lines of harness are considered, see Figure 23. Each line departs from the SVM top plate node, intercept the VGs and then the TOB. Further details are reported in [RD2] |

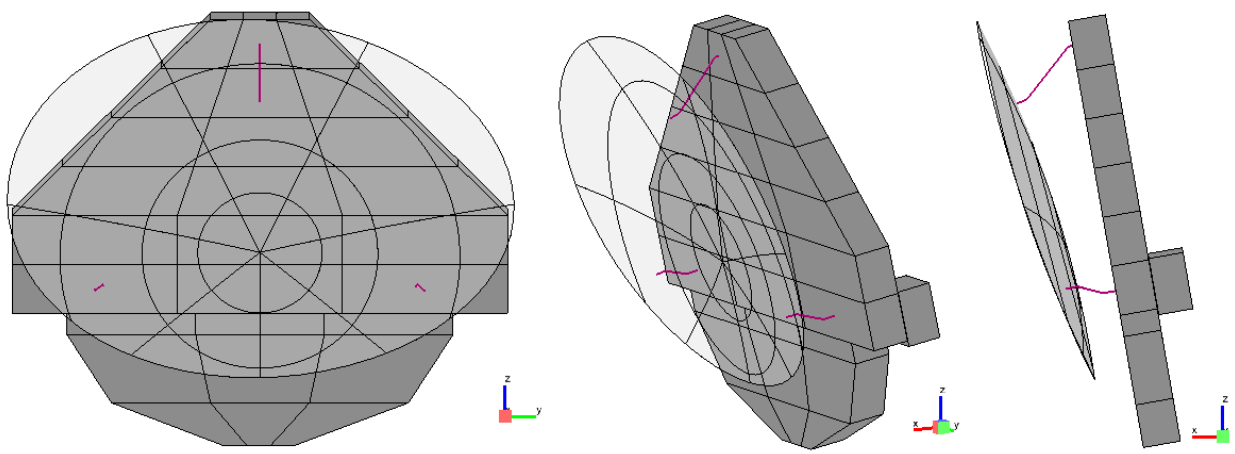

***Figure 21: Three views of the M1 and TOB showing the three conductors representing the mechanical supports of the M1 on the TOB. The M1 geometry is shown transparent for clarity.***

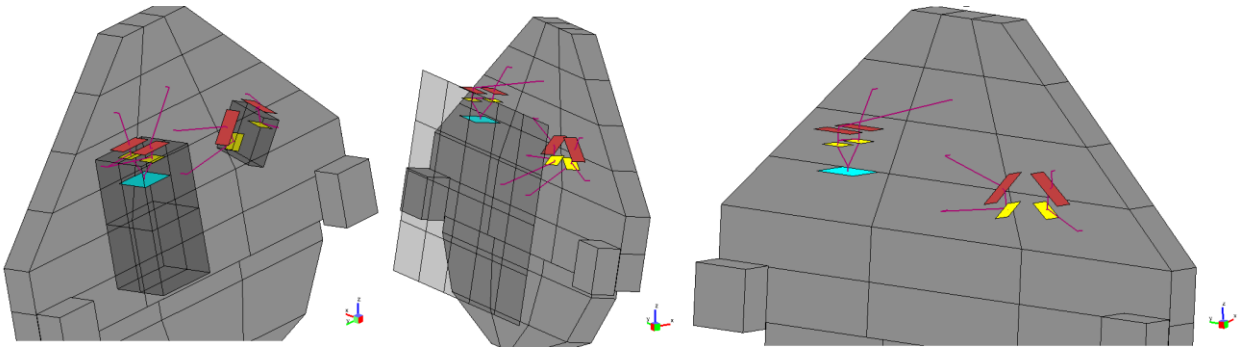

***Figure 22: User-defined conductors between detectors, CFEEs, TOB and cold references (JT cold end for AIRS and Instrument radiator for FGS/NIRP). In the central view the Instrument radiator is shown transparent: it is possible to see the conductors between the FGS/NIRP detector and the radiator.***

### 3.3.2 Harness budgets

In the present issue of the ARIEL PLM TMM the contribution of the harness is evaluated by using defined conductors with an associated thermal conductance that simulate the heat leaks at each stage (plus an extra margin). The harness is assumed as split in two main branches both running from the SVM to the OB, dissipating on each V-Groove (see Figure 23). The conductance of each thermal step and for each branch is G = 0.002 W/K. In total, each thermal step (SVM-VG1, VG1-VG2, VG2-VG3 and VG3-TOB) is connected with a total G=0.004 W/K.

A more detailed description of the assumptions on the PLM harness configuration is reported in [RD2].

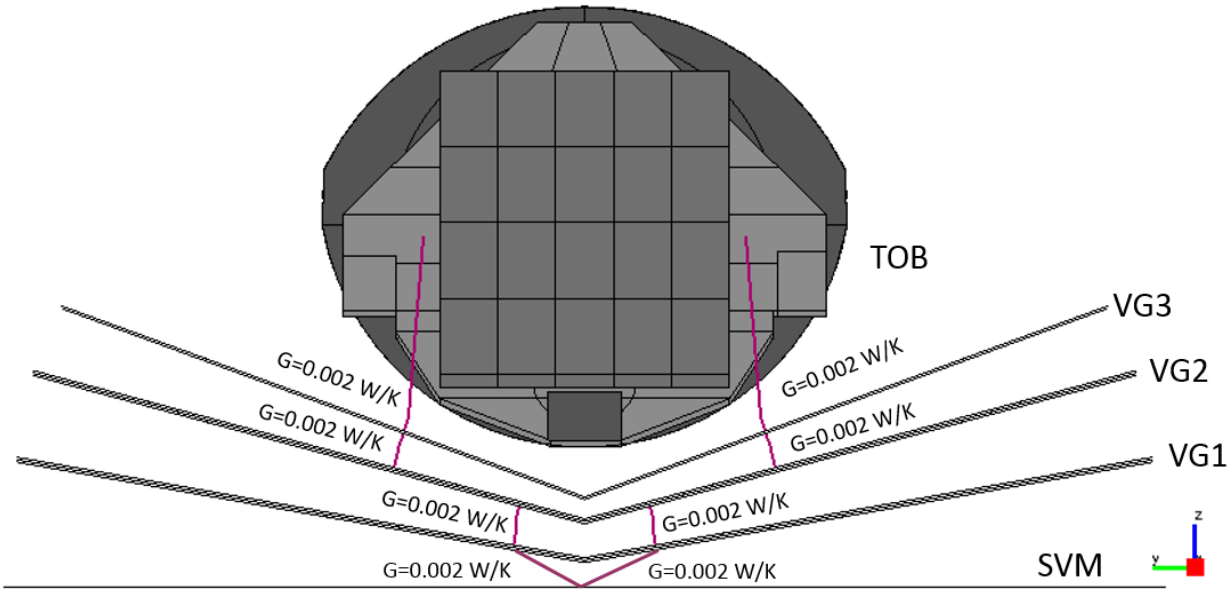


***Figure 23: PLM harness simulating conductors layout.***

### 3.3.3 Boundary conditions and Thermal-analysis cases

In order to fully characterize the PLM system thermal performance, different boundary conditions are considered. For each significant set of boundary conditions associated with a scenario (radiative case) a thermal-analysis case is created and solved. The Table 15 and Figure 24 report the power boundary conditions considered for the nominal operation cases. The table includes the power dissipation of the instrument detectors and the CFEEs, the heat lift of the JT cold end. The power dissipation on the VG3 (last item in the table) refers to the power intercepted by the VGs for pre-cooling of the working fluid of the JT

active cooler (as per RAL estimation). In all analysis cases this heat load is totally allocated in one node of VG3 at the intersection of one of the rear bipod leg (the node 12621 of the VG3, colored in red in Figure 24). This represents a worst case condition: the load is fully dissipated on one node on the last V-Groove only (TBC) and the position of this node, right at the intersection with the bipod, increases the power leaked to the bench.

The JT cooler heat exchanger is, at this stage, simulated as a diffusion node with a fixed heat lift (negative power) with no assumptions on two-phase characteristics. Once a cooling power map and two-phase flow properties will be available a more realistic simulation of the JT heat exchanger will be implemented. Even if the baseline cooler for ARIEL can be sized to be capable of producing a cooling power up to 50 mW or more, for thermal analysis purposes an extra margin of 25% has been assumed on this number. In the present thermal design of the PLM, the JT cold tip balance temperature reaches the 35-36K range with 37.5 mW of heat lift produced.

The AIRS SCA's active load assumed for the thermal analysis (Table 3) is 15 mW (with margin) but that number already includes the parasitic leaks (struts, harness) to the FPA that are the dominant contribution over the actual electrical dissipation (see [RD4] AIRS Design Description Document). The TMM computes independently the heat leaks due to the struts (the main parasitic load ~6 mW). For this reason in the TMM the dissipation associated to each AIRS SCA's is 10 mW, which corresponds to an extra 35% margin assumed over the actual active load of the detectors stage.

***Table 15: Boundary heat loads at nominal operations.***

| Node | Power |
|---|---|
| AIRS detector 1 | 10 mW |
| AIRS detector 2 | 10 mW |
| FGS/NIRP detector 1 | 20 mW |
| FGS/NIRP detector 2 | 20 mW |
| AIRS CFEE 1 | 100 mW |
| AIRS CFEE 2 | 100 mW |
| FGS/NIRP CFEE 1 | 100 mW |
| FGS/NIRP CFEE 2 | 100 mW |
| JT cold end | -37.5 mW |
| Node 12621 of VG3 | 320 mW |

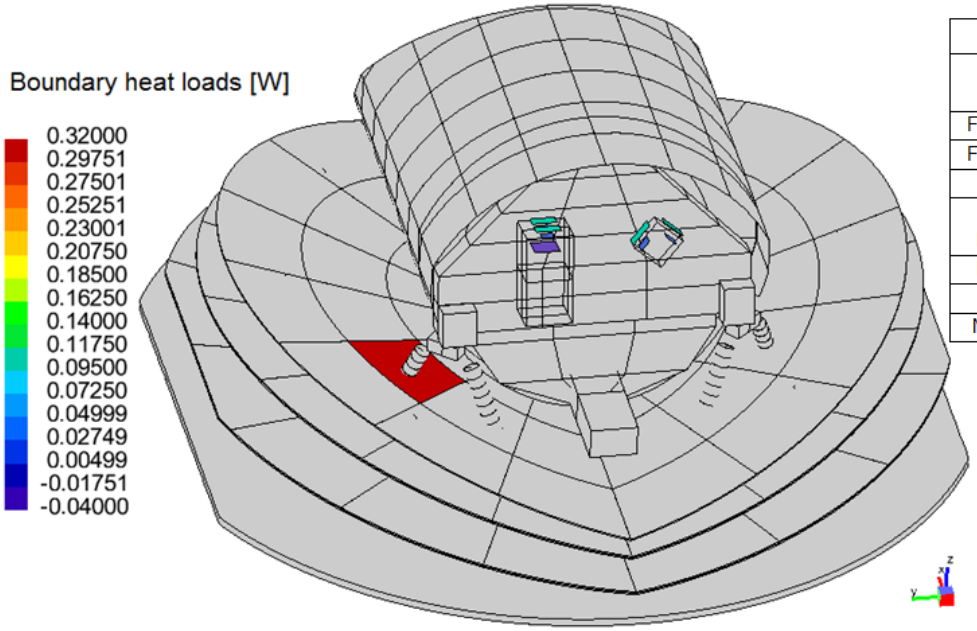


***Figure 24: Boundary heat loads associated to the corresponding nodes***

Temperature boundary conditions are applied on both surfaces of the SVM/PLM I/F (conductive and radiative) to fully represent the thermal coupling of the PLM with the SVM. All PLM nodes are represented as diffusion nodes. Only in a single case, a fixed temperature is applied to the M1, in order to find the power needed for the decontamination process during the in-flight cool down. Table 16 reports the solved analysis cases with the associated radiative case and boundary conditions.

***Table 16: Studied analysis cases.***

| ***Analysis case*** | ***Radiative case*** | ***Boundary conditions*** | ***Type of solution*** |
|---|---|---|---|
| **Cold case at nominal operational** | Earth-Sun L2 point | SVM top plate @ 270K (fixed)<br>SVM Radiative shield @ 180K (fixed)<br>Powers in Table 15 | Steady-state |
| **Hot case at nominal operational** | Earth-Sun L2 point | SVM top plate @ 290K (fixed)<br>SVM Radiative shield @ 200K (fixed) | Steady-state |

| | | | |
|---|---|---|---|
| | | Powers in Table 15 | |
| **SVM temperature variation during observation (instantaneous change)** | Earth-Sun L2 point | Initial temperature: hot case steady-state temperature<br>SVM top plate from 290K to 280K<br>*instantaneous change at t=0s*<br>SVM Radiative shield @ 200K (fixed)<br>Powers in Table 15 | Transient<br>(10 hours) |
| **SVM temperature variation during observation (linear change)** | Earth-Sun L2 point | Initial temperature: hot case steady-state temperature<br>SVM top plate from 290K to 280K<br>*linear variation over 10 hours*<br>SVM Radiative shield @ 200K (fixed)<br>Powers in Table 15 | Transient<br>(10 hours) |
| **Preliminary PLM cool-down** | Earth-Sun L2 point | Initial temperature: all nodes @ 290 K<br>SVM top plate @ 290 K (fixed) | Transient<br>(30 d) |
| **Preliminary PLM decontamination** | Earth-Sun L2 point | M1 @ 170 K (fixed)<br>SVM top plate @ 290K (fixed) | Steady-state |
| **Preliminary PLM decontamination** | Earth-Sun L2 point | Initial temperature: all nodes @ 290 K<br>SVM top plate @ 290 K (fixed)<br>Power @ M1 by a PID controller | Transient<br>(15 d) |
| **PLM exposed to each Sun vector** | LEOP for each considered Sun vector | SVM top plate @ 290K (fixed) | Steady-state |
| **PLM exposed to the worst case Sun vector** | LEOP with the worst case Sun vector | Initial temperature: all nodes @ 290 K<br>SVM top plate @ 290K (fixed) | Transient<br>(1 hour) |

# 4 PLM TMM/GMM MODEL RESULTS

## 4.1 NOMINAL OPERATIONS THERMAL CASE

### 4.1.1 Nominal Operations Steady-state Analyses

Table 17 shows the solved steady-state temperatures of the cold and hot case for the nominal conditions, corresponding to the S/C orbiting at the Earth-Sun L2 point in routine operations attitude and loads conditions. The Cold and Hot Cases are different just for the fixed boundary temperatures applied at the SVM/PLM I/F.

***Table 17. Steady-state temperatures for the cold and hot case in nominal conditions.***

| PLM Unit | Cold case T [K] | Hot case T [K] | Req [K] | Margin [K] |
|---|---|---|---|---|
| *SVM top plate (fixed boundary temperature)* | *270.00* | *290.00* | - | - |
| *SVM Radiative shield (fixed boundary temperature)* | *180.00* | *200.00* | - | - |
| VG1 | 148.6 | 158.1 | 180 | 10 |
| VG2 | 97.4 | 103.1 | 120 | 10 |
| VG3 | 55.1 | 56.6 | 70 | 10 |
| Telescope M1 | 49.4 | 50.4 | 70 | 10 |
| Telescope M2 | 48.8 | 49.8 | 70 | 10 |
| Telescope Baffle | 48.2 | 49.1 | 60 | 10 |
| TOB | 49.6 | 50.5 | 60 | 10 |
| Instrument Box | 49.6 | 50.5 | 60 | 10 |
| FGS/NIRP CFEEs | 50.1 | 51.0 | 70 | 10 |
| FGS/NIRP detectors | 49.5 | 50.3 | 70 | 10 |
| Instrument radiator | 48.9 | 49.8 | 60 | 10 |
| AIRS CFEEs | 50.1 | 51.0 | 62 | 10 |
| AIRS detectors | 35.1 | 36.0 | 42 | 5 |
| JT cold end | 34.9 | 35.9 | 40 | 5 |

In the table above, the temperature results are compared to the requirements with the margins to be assumed at this stage of the design process. The temperature of all passively and actively cooled units are fully compliant to the requirements including margins. The unit temperatures are graphically shown in the next figures, comparing the Cold and Hot cases: general views of the PLM are compared in Figure 25, while Figure 26 and Figure 27 show the details of the coldest units in both cases.

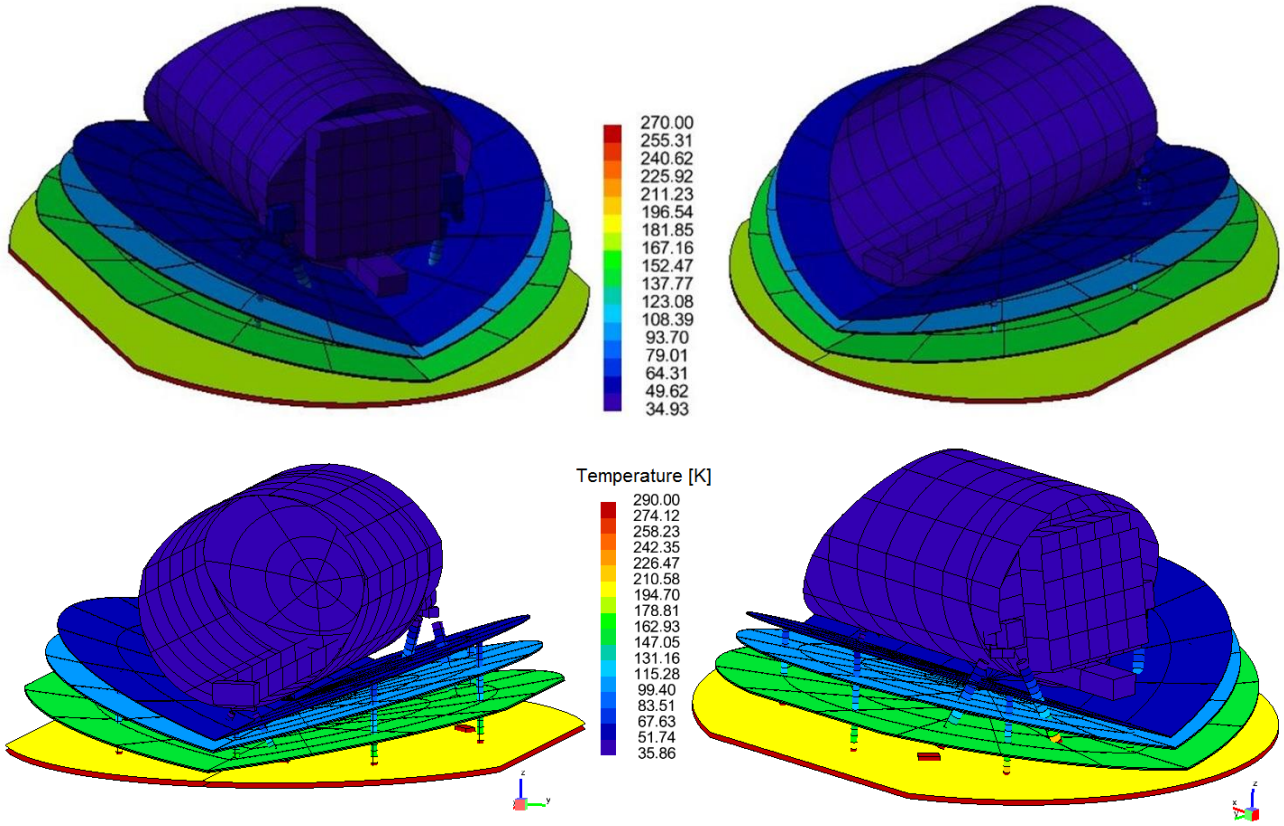


***Figure 25: Cold Case (upper panel) and Hot Case (lower panel) steady-state results in nominal conditions, general views of the PLM model.***

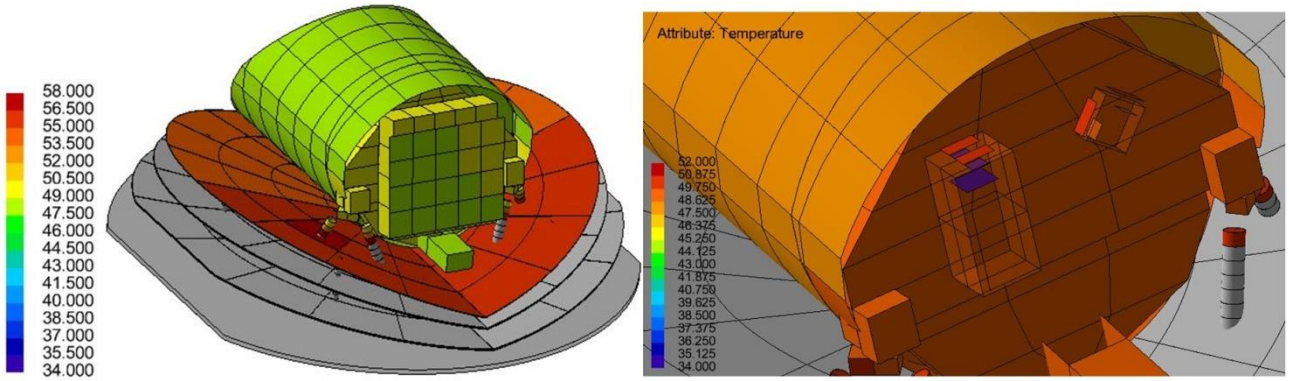


***Figure 26: Cold case steady-state results in nominal conditions, detailed views of the cold PLM. Left view shows the radiator, OB and baffle temperatures. Right side: the module boxes are hidden in transparency to show AIRS and FGS/NIRP CFEEs, detectors and the JT cold end.***

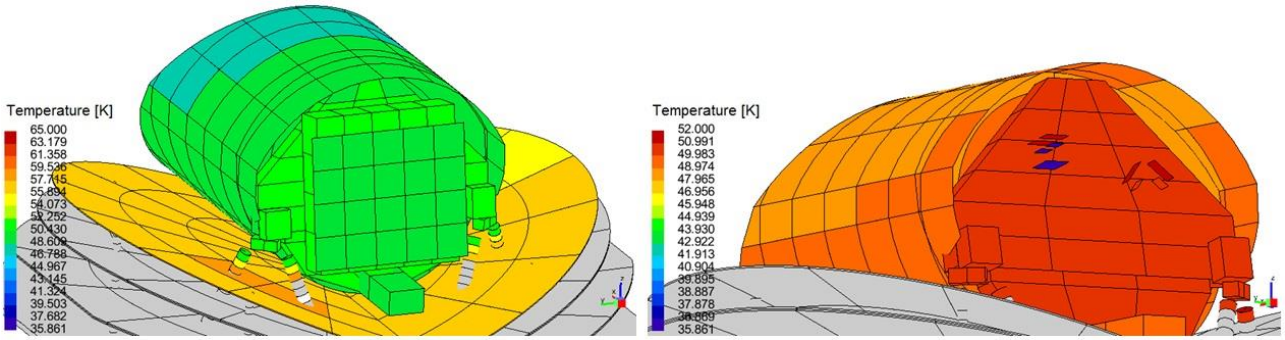


***Figure 27: Hot case steady-state results in nominal conditions, detailed views of the cold PLM. Left view shows the radiator, OB and baffle temperatures. Right side: the module boxes are hidden to show AIRS and FGS/NIRP CFEEs, detectors and the JT cold end.***

Figure 28 reports a detailed view of the Telescope Assembly in the Cold Case, to show the thermal uniformity reached by the passive cooling. M1 maximum gradient is lower than few mK.

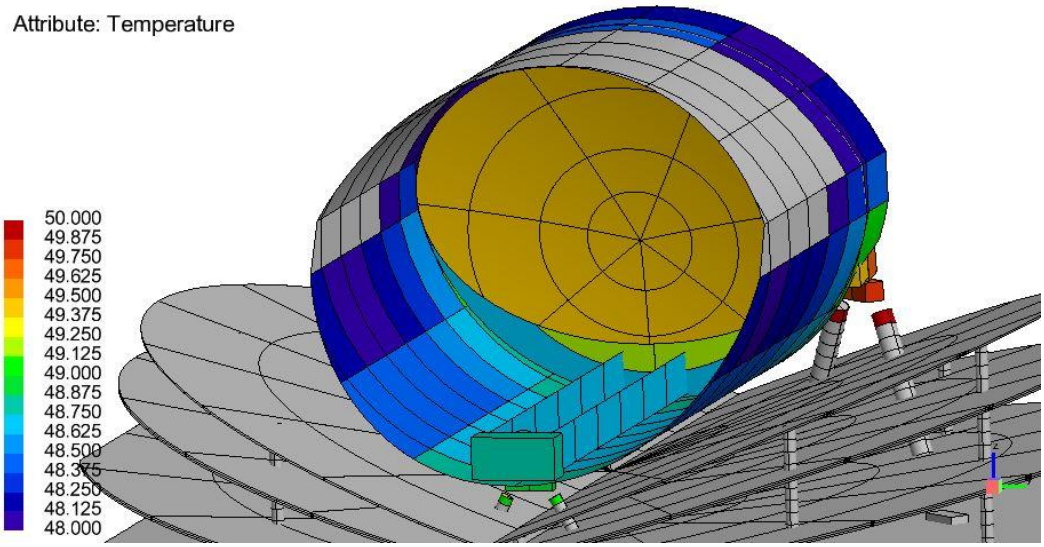


***Figure 28: Telescope Assembly nodes temperature in the Cold Case***

The G/TMM performances in terms of heat fluxes to/from the PLM units and rejection capabilities of the passive cooling radiators are summarized in the following table.

***Table 18: Heat exchange at the main internal interfaces and between units for Cold and Hot cases in nominal conditions.***

| PLM IF main heat flux | Cold case [W] | Hot case [W] |
|---|---|---|
| VG1 heat rejection to space | 7.6 | 9.8 |
| VG2 heat rejection to space | 1.1 | 1.4 |
| VG3 heat rejection to space | 1.0 | 1.1 |
| Telescope Baffle heat rejection to space | 0.7 | 0.8 |
| Instrument radiator heat rejection to space | 0.096 | 0.103 |
| Optical Bench heat rejection to space | 0.037 | 0.039 |
| Conductive heat flux from bipods' heads to TOB | 0.12 | 0.13 |
| Conductive heat flux from TOB to Mirror 1 | 0.010 | 0.012 |
| Conductive heat flux from TOB to Baffle | 0.350 | 0.360 |
| Conductive heat flux from CFEEs (both FGS and AIRS) to TOB | 0.37 | 0.36 |
| Conductive heat flux to FGS detectors | 0.017 | 0.019 |
| Conductive heat flux to AIRS detectors | 0.017 | 0.017 |

The V-Groove 3 is capable of rejecting more than 1W at a temperature of 55K, while the telescope baffle and the instrument radiator dissipate to space, respectively, 0.7 W and 0.1W.

The loads to the Instrument interfaces are evaluated by balancing the input/output heat fluxes to/from each node through all conductors. The most relevant heat loads and exchanges for the main thermal interfaces are reported in the following tables.

**SVM platform: conductive interface**

| Heat flow | Cold case [W] | Hot case [W] |
|---|---|---|
| Conductive to bipods | 22.07 | 27.78 |
| Conductive to supports | 4.05 | 4.95 |
| Radiative to SVM radiative shield | 26.88 | 34.49 |
| Radiative to cold space | 12.36 | 16.45 |

***Table 19: Most relevant SVM top plate heat exchange and loads for cold and hot case in nominal conditions.***

**SVM MLI shield: radiative interface**

| Heat flow | Cold case [W] | Hot case [W] |
|---|---|---|
| Radiative from bipods | 4.54 | 5.74 |
| Radiative from supports | 1.02 | 1.13 |
| Radiative from SVM top plate | 26.88 | 34.49 |
| Radiative to cold space | 12.14 | 18.50 |

***Table 20: Most relevant SVM radiative shield heat exchange and loads for cold and hot case in nominal conditions.***

**V-Groove 1**

| Heat flow | Cold case [W] | Hot case [W] |
|---|---|---|
| Conductive from SVM (through harness) | 0.48 | 0.52 |
| Radiative from SVM radiative shield | 1.43 | 2.46 |
| Total from bipods | 6.78 | 8.08 |
| Total from supports | 0.09 | 0.12 |
| Conductive to VG2 (through harness) | 0.21 | 0.22 |
| Radiative to VG2 | 1.14 | 1.43 |
| Radiative to cold space | 7.63 | 9.77 |

***Table 21: Most relevant VG1 heat exchange and loads for cold and hot case in nominal conditions.***

**V-Groove 2**

| Heat flow | Cold case [W] | Hot case [W] |
|---|---|---|
| Conductive from VG1 (through harness) | 0.21 | 0.22 |
| Radiative from VG1 | 1.14 | 1.43 |
| Total from bipods | 0.35 | 0.42 |
| Total from supports | 0.02 | 0.02 |
| Conductive to VG3 (through harness) | 0.17 | 0.18 |
| Radiative to VG3 | 0.38 | 0.46 |
| Radiative to cold space | 1.13 | 1.41 |

***Table 22: Most relevant VG2 heat exchange and loads for cold and hot case in nominal conditions.***

**V-Groove 3**

| Heat flow | Cold case [W] | Hot case [W] |
|---|---|---|
| Conductive from VG2 (through harness) | 0.17 | 0.18 |
| Radiative from VG2 | 0.38 | 0.46 |
| Total from bipods | 0.49 | 0.56 |
| Total from supports | 0.15 | 0.17 |
| Conductive to TOB (through harness) | 0.02 | 0.02 |
| Radiative to Baffle (TOB, Instrument Box, Radiator) | 0.29 (0.01, 0.01, 0.01) | 0.34 (0.01, 0.01, 0.01) |
| Radiative to cold space | 0.98 | 1.08 |

***Table 23: Most relevant VG3 heat exchange and loads for cold and hot case in nominal conditions.***

**TOB**

| Heat flow | Cold case [W] | Hot case [W] |
|---|---|---|
| Conductive from CFEE | 0.37 | 0.36 |
| Total from bipods | 0.12 | 0.13 |
| Conductive to detectors | 0.02 | 0.02 |
| Total to Baffle | 0.35 | 0.36 |
| Total to Mirror 1 | 0.01 | 0.01 |
| Total to Instrument Box | 0.04 | 0.05 |
| Radiative to cold space | 0.04 | 0.04 |

***Table 24: Most relevant TOB heat exchange and loads for cold and hot case in nominal conditions.***

**Baffle**

| Heat flow | Cold case [W] | Hot case [W] |
|---|---|---|
| Radiative from M1 | 0.003 | 0.003 |
| Total from bipods | 0.05 | 0.05 |
| Total from TOB | 0.35 | 0.36 |
| Total from Instrument Box | 0.003 | 0.05 |
| Radiative to cold space | 0.71 | 0.77 |

***Table 25: Most relevant Baffle heat exchange and loads for cold and hot case in nominal conditions.***

**Instrument Radiator**

| Heat flow | Cold case [W] | Hot case [W] |
|---|---|---|
| Radiative from SVM radiative shield | 0.001 | 0.002 |
| Conductive from FGS/NIRP detectors | 0.05 | 0.06 |
| Total from Instrument Box | 0.03 | 0.03 |
| Radiative to cold space | 0.10 | 0.10 |

***Table 26: Most relevant instrument radiator heat exchange and loads for cold and hot case in nominal conditions.***

The **JT cold end** heat balance is always 37.5 mW because this is a fixed boundary condition. The parameter that shows the heat balance performances of the JT heat exchanger is the equilibrium temperature of the cold end (and of the AIRS detectors'). This temperature is around 36K or below in both cases.

The tables above provide an indication of the efficiency and performances of the ARIEL PLM passive design. The V-Groove 3 is capable of rejecting more than 1 W at a temperature of 55K (15K below the requirement), while the telescope baffle and the instrument radiator dissipate to space, respectively, 0.7 W and 0.1 W at temperatures below the requirements.

### 4.1.2 SVM/PLM I/F temperature variation, transient analysis

Thermal stability is one of the key issue of the ARIEL PLM thermal design. For this reason, an analysis case is computed to check the impact of a temperature variation of the SVM platform conductive IF on the PLM during a nominal scientific observation run (10 hours). The required stability level at this interface [AD2] is a 6 K (± 3 K) peak-to-peak maximum oscillation. To evaluate a worst case, a 10 K change is assumed in this analysis run. The SVM/PLM I/F variation is simulated by changing the boundary temperature of the SVM top plate during the transient solution routine. The other boundary conditions (SVM radiative shield @ 200 K and powers in Table 15) remain unchanged during the transient simulation, that starts with the system in the Hot Case steady-state conditions. The steady-state solver is then run in advance to the transient routine in order to take all nodes of the model at the hot case steady-state temperatures. At that point, two analysis cases are simulated:

1. Sudden change: at the beginning of the transient routine (t=0 s), the boundary temperature of the SVM top plate is changed instantaneously from 290 K to 280 K. The transient solver runs for a 10 hours simulation.

2. Linear change: the boundary temperature of the SVM top plate changes linearly from 290 K to 280 K during the whole duration of the transient routine (10 hours, 1 K per hour).

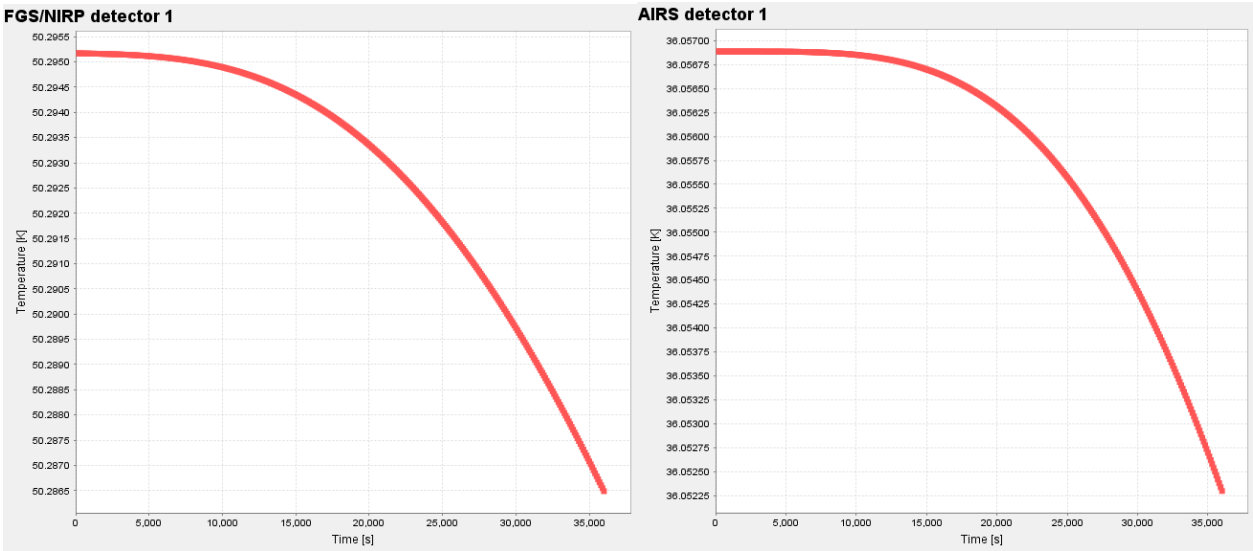


***Figure 29: FGS/NIRP and AIRS detector temperature variation over 10 hours for an instantaneous change of the boundary temperature of the SVM top plate from 290 K to 280 K, all thermal control loops are deactivated. The Y axis scale is 9 mK for the FGS detectors and 5 mK for the AIRS.***

Figure 29 shows the transient temperature results of the detector #1 of the FGS/NIRP and AIRS in the instantaneous change (first case). The total change of the FGS and AIRS detectors temperature in 10 hours is, respectively, 9 mK and 4.75 mK. Figure 30 shows the transient temperatures of the coldest and hottest nodes of the primary mirror geometry in the same first case. The total change of both nodes is less than 2 mK.

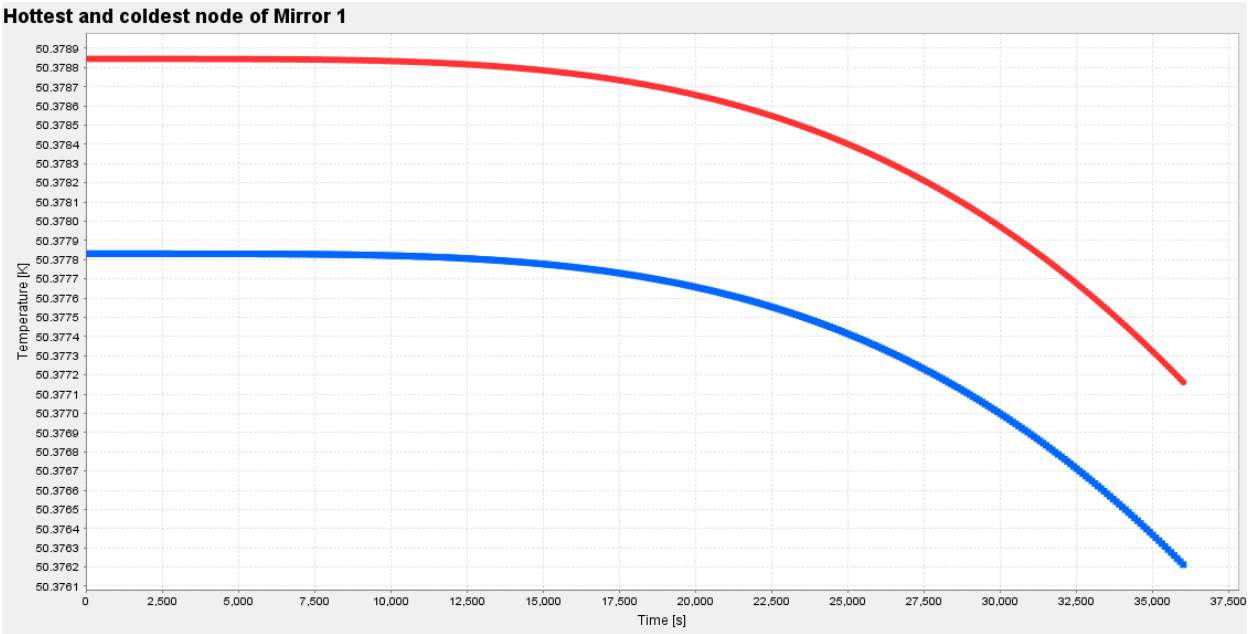


***Figure 30: Temperature variation of the hottest and coldest node of the M1 geometry over 10 hours for an instantaneous change of the boundary temperature of the SVM top plate from 290 K to 280 K. M1 thermal control system is off. The scale of the Y axis is 3 mK.***

Figure 31 and Figure 32 show the same plots for the linear change (second case), when a smoother temperature change is imposed at the interface. The total change of the FGS and AIRS detectors temperature in 10 hours is, respectively, 2.5 mK and 1 mK. The total change of the M1 nodes is less than 0.5 mK.

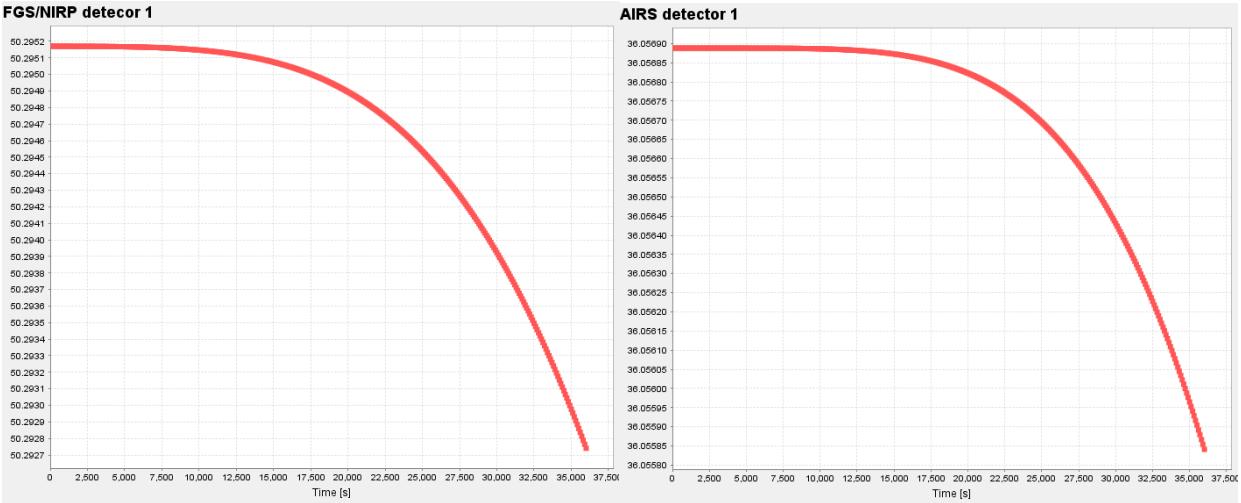


***Figure 31: FGS/NIRP and AIRS detector temperature variation over 10 hours for a linear change of the boundary temperature of the SVM top plate from 290 K to 280 K in 10 hours. The Y axis scale is 2.7 mK on the left panel and 1.2 mK on the right.***

The instabilities transmitted to the FGS and AIRS detectors and to the primary mirror by a 10 K peak-to-peak variation at the SVM to PLM conductive interface during a 10 hours observation run are well below the required level of stability for those units.

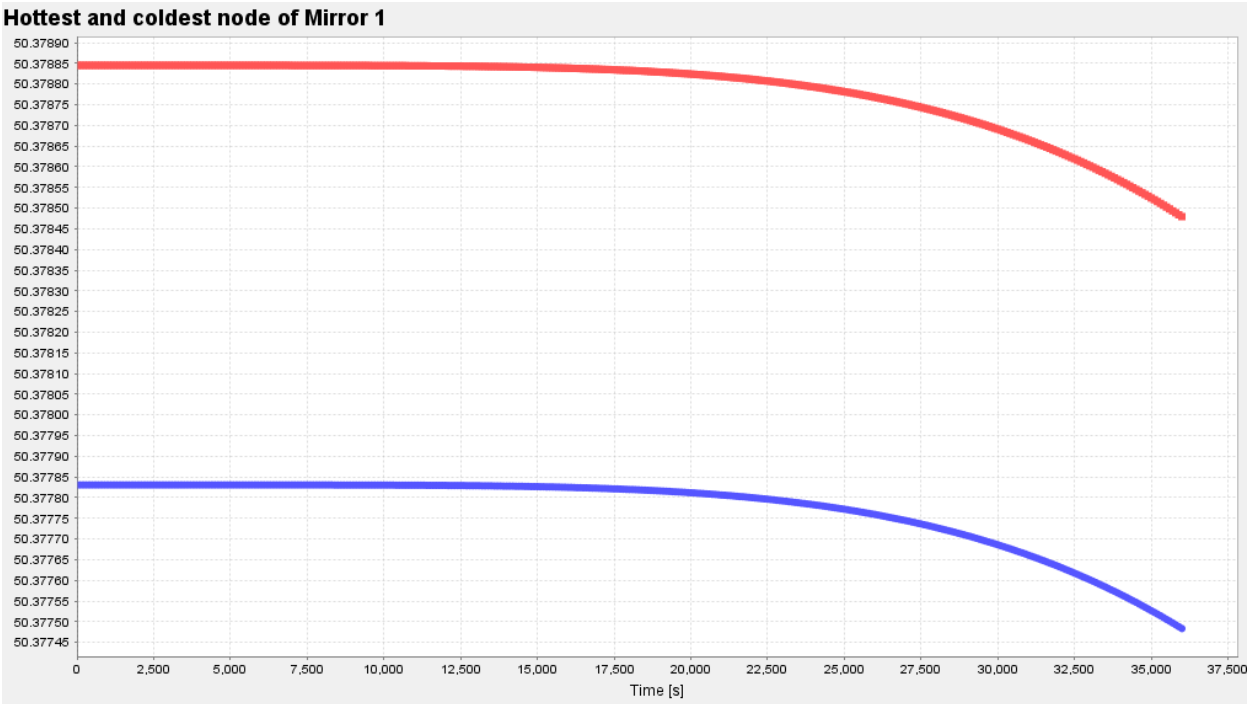


***Figure 32: Temperature variation of the hottest and coldest node of the M1 geometry over 10 hours for a linear change of the boundary temperature of the SVM top plate from 290 K to 280 K in 10 hours. Y scale is 1.5 mK.***

### 4.1.3 Detectors TCS Stability Preliminary Analysis

Stable conditions and systematic errors control during observations are key requirements for the scientific objectives of ARIEL. For this reason, thermal stability is another key driver of the mission design. There are two possible thermal noise sources in the PLM: the radiators (V-Grooves, telescope bench and instrument box) and the cooler cold end. The main cause of fluctuations on a radiator facing the cold sky is due to orbital changes of the Solar Aspect Angle (SAA) related to flight dynamics following the mission scanning

strategy (on timescales of 10 hours or so) or seasonal variations (typically on longer periods like weeks, months, years). Experience on previous missions (Planck), testing and simulations shows that such low frequency oscillations can be controlled under 200 mK over timeframes of 10 hours to avoid the thermal background stability becoming a major contributor in the instrument noise budget. The most significant temperature variation can happen when the Sun aspect angle changes while slewing to observe a new science target. Constraints on the maximum slew angle between successive targets (<25°) are set to limit the SAA changes and the induced temperature variation to less than 10K in the SVM top floor. This variation is damped by the thermal capacitance and shielding of the PLM, to a level that can be evaluated by analysis and simulations.

In a JT cooler, instabilities at the reference heat exchanger temperature are due to compressor modulation, with its typical high frequency spectrum (30-40Hz range), to cold-end internal mass flow 1- or 2-phase dynamics (on the order of tens of seconds) and to precooling stage variations (low frequency).

Thermal stability of the optical modules directly connected to the TOB (FGS/NIRP and AIRS) is not expected to be a major concern given the typical instabilities of passive radiators in L2 either on the timescales of the detectors average exposure or on the seasonal. Even in the case of few hundreds of mK peak to peak fluctuations every several hours (10000 s time scale), the thermal inertia of the instrument bench and modules is enough to damp them well below the required 0.5 K peak to peak.

The detectors are directly connected to their temperature reference and the level of transmitted fluctuations could be at the limit of the required values. Since FPA stability is a key issue for instrumental performance, a careful design of a proper thermal control system is needed. This is achieved by a combination of passive and active systems as reported in Chapter 2. To verify the functionality of the active control stages design on the ARIEL detectors, analytical studies correlated with a set of transient simulations have been carried out.

If periodical thermal instabilities can be approximated with a sinusoidal function and imposed at the relevant interfaces, then the temperature fluctuations transmitted passively at the sensitive stages (the TCS for example) connected to the thermal noise source can be approximated by

$$\Delta T_{TCS} \cong \frac{\Delta T_0}{\sqrt{1+\omega^2 R_{TCS}{}^2 C^2{}_{TCS}}} \cos(\omega t + \varphi)$$

where $C_{TCS}$ is the thermal capacitance of the stage, $R_{TCS}=1/G_{TCS}$ is the resistance between the TCS and the source of the instabilities (cold radiator or the cooler cold end) and $\omega$ is the pulsation of the oscillations. The damping factor RC depends on the thermal mass of the stage and on the thermal break with the noise source. Since the thermal inertia of the Temperature Control Stages designed for the detectors is very small, the thermal resistance becomes the key parameter for oscillations passive damping. The conductance value between the detector TCS and its temperature reference is selected on the basis of a trade-off between the detectors operating temperature and the minimum power needed to achieve thermal control at the TCS.

In the next table are reported some conservative predictions of the possible fluctuations expected on the cold radiator stage and at the cooler cold end heat exchangers level based on what observed for radiators orbiting L2 in previous missions like Planck. Planck scanning strategy allowed the spacecraft to constantly maintain a low optimal solar aspect angle. The case for the ARIEL flight dynamics will likely push the mission to higher SAA values. This would reflect in possible oscillations at the radiator stages at each re-pointing step, inducing also oscillations in the cooler cold end: a conservative estimation of the pre-cooling stage induced fluctuations on the cooler is 0.01K/K. As this first analysis that has the objective of providing a safe figure for the thermal oscillations at various stage, it has been decided to assume conservative numbers in terms of expected oscillation frequency spectrum. These assumptions are shown in the first three columns of the following tables.

***Table 27: Preliminary analysis of worst case temperature fluctuation spectrum at Instrument Radiator***

| Time (s) | Frequency (Hz) | p-p ΔT (K) at radiator | ΔT at 50K TCS (K) | ΔT at 50K DS (K) | Q_tcs max (W) | Q_tcs ave (W) |
|---|---|---|---|---|---|---|
| 10 | 0.1 | 0.002 | 3.181E-05 | 1.129E-06 | 1.909E-06 | 1.273E-06 |

| | | | | | | |
|---|---|---|---|---|---|---|
| 100 | 0.01 | 0.005 | 0.0008 | 0.0003 | 4.550E-05 | 3.033E-05 |
| 1000 | 0.001 | 0.01 | 0.0048 | 0.0046 | 0.0003 | 0.0002 |
| 10000 | 0.0001 | 0.1 | 0.0500 | 0.0500 | 0.0030 | 0.0020 |

***Table 28: Preliminary analysis of worst case temperature fluctuation spectrum at 40K stages***

| Time (s) | Frequency (Hz) | p-p ΔT at cold end (K) | ΔT at 40K TCS (K) | ΔT at 40K DS (K) | Q_tcs max (W) | Q_tcs ave (W) |
|---|---|---|---|---|---|---|
| 10 | 0.1 | 0.00002 | 0.00001 | 7.933E-07 | 1.768E-08 | 9.519E-08 |
| 100 | 0.01 | 0.00005 | 0.000025 | 1.557E-05 | 4.420E-07 | 1.868E-06 |
| 1000 | 0.001 | 0.0001 | 0.00005 | 4.961E-05 | 8.707E-06 | 5.953E-06 |
| 10000 | 0.0001 | 0.001 | 0.0005 | 0.0005 | 0.0004 | 0.0001 |

In these tables the timescales and frequencies of the expected peak to peak fluctuations at the noise source (radiator or cold end) are then compared to the oscillations transmitted to the relative TCS and DS stage of the AIRS channel. It is clear from this very simple analysis how the thermal design of the units allows for an efficient passive filtering of most of the higher frequency noise. From this follows that all possible oscillations generated in the cooler are damped to negligible levels by the thermal inertia and resistance of the systems. Typical compressor frequencies are in the tens of Hz ranges while noise generated in the cold end due to mass flow instabilities typically happens over tens of second time scales with few mK variations. The last two columns report the maximum and average proportional control power needed to control the transmitted fluctuations well below the required level.

### 4.1.4 Preliminary cool-down simulation

This analysis case provides a preliminary estimation of the in-flight cool-down time required by the PLM. The model is exposed to deep space with the nominal attitude, the initial temperature of all nodes is 290 K.

The fixed boundary temperature of the SVM plate of 290 K is the only boundary condition applied. Figure 33 shows the transient solution for principal PLM units for 30 days (2592000 s). After 25-30 days the transitory process is practically concluded and the system can be assumed to be in nearly steady state. Table 29 reports the final temperatures of the main units after 30 days. The simulated process is fully passive. Once the heat lift map of the JT cold end will be available, the effect of the cooler activation and other heat loads that could be present in the PLM at that stage, if any, will be introduced in the simulation.

The cooldown curve shows that most of the passive cool down is completed within the first week or so. VG1 and VG2 reach their operating temperature ranges within 3 days, while VG3 takes twice this time. After a month the passive cooldown can be considered at steady-state. This curves indicate cool-down times very similar to what has been observed on the Planck spacecraft after launch and orbit to L2 injection.

***Table 29: Temperatures of the main units after a cool-down simulation of 30 days.***

| Unit | Temperature [K] |
|---|---|
| *SVM top plate (fixed boundary temperature)* | *290.0* |
| SVM Radiative shield | 224.0 |
| VG1 | 163.8 |
| VG2 | 105.6 |
| VG3 | 53.7 |
| Telescope M1 | 45.1 |
| Telescope M2 | 45.3 |
| Telescope Baffle | 44.6 |
| TOB | 45.1 |

| | |
|---|---|
| Instrument Box | 45.1 |
| FGS/NIRP CFEEs | 45.1 |
| FGS/NIRP detectors | 44.6 |
| Instrument radiator | 44.4 |
| AIRS CFEEs | 45.1 |
| AIRS detectors | 45.1 |
| JT cold end | 45.1 |

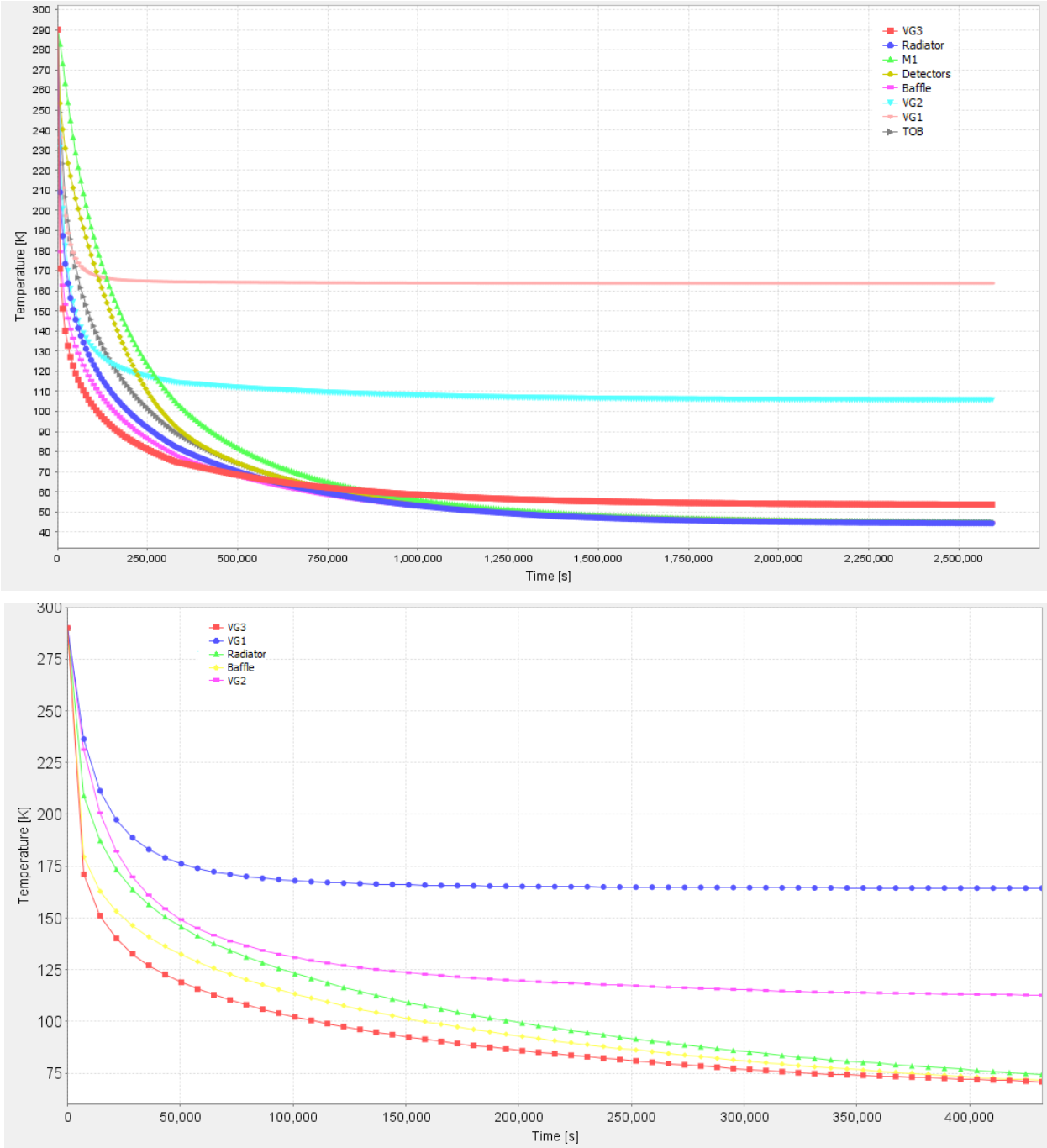


***Figure 33: 30 days PLM cool-down simulation. The PLM is in shade from the Sun at the Earth-Sun L2 point, the SVM top plate is kept at fixed boundary temperature of 290 K. Top panel: overview of the 30 days cool-down simulation result. Bottom panel: zoomed view of the first 5 days of cool-down.***

### 4.1.5 Preliminary PLM Decontamination analysis

In order to evaluate the power needed for telescope decontamination, the activation of the heaters during the cool-down of the telescope assembly has been simulated. The mirrors set point of the decontamination temperature is 170 K. Once the telescope reaches 170 K, a set of heaters on the telescope are turned on to maintain the temperature around this value with a proportional control loop. In this preliminary analysis only the Mirror 1 (M1 geometry in the Workbench) is considered in the decontamination process, as the main contribution to the power needed will be required for the much heavier primary mirror. The power needed for the M2 and M3 is included in the margin considered for this estimation (50%).

At first, the maximum decontamination power is estimated at first order with a simple steady-state analysis by considering the radiative case at the Earth-Sun L2 point, the SVM top plate at fixed temperature of 290 K and the M1 as a fixed boundary at the temperature of 170 K. From the steady-state results, the total power (radiative and conductive) balance of the M1 at 170 K with the rest of the model and environment is 27.2 W. This means that in nominal conditions, once the mirror is cold at 50K, the power required to raise its temperature and keep it around 170K is nearly 30 W (45 W including 50% margin). This can be a useful information if the decontamination process is expected to be executed not only during cooldown but also during mission scientific operations

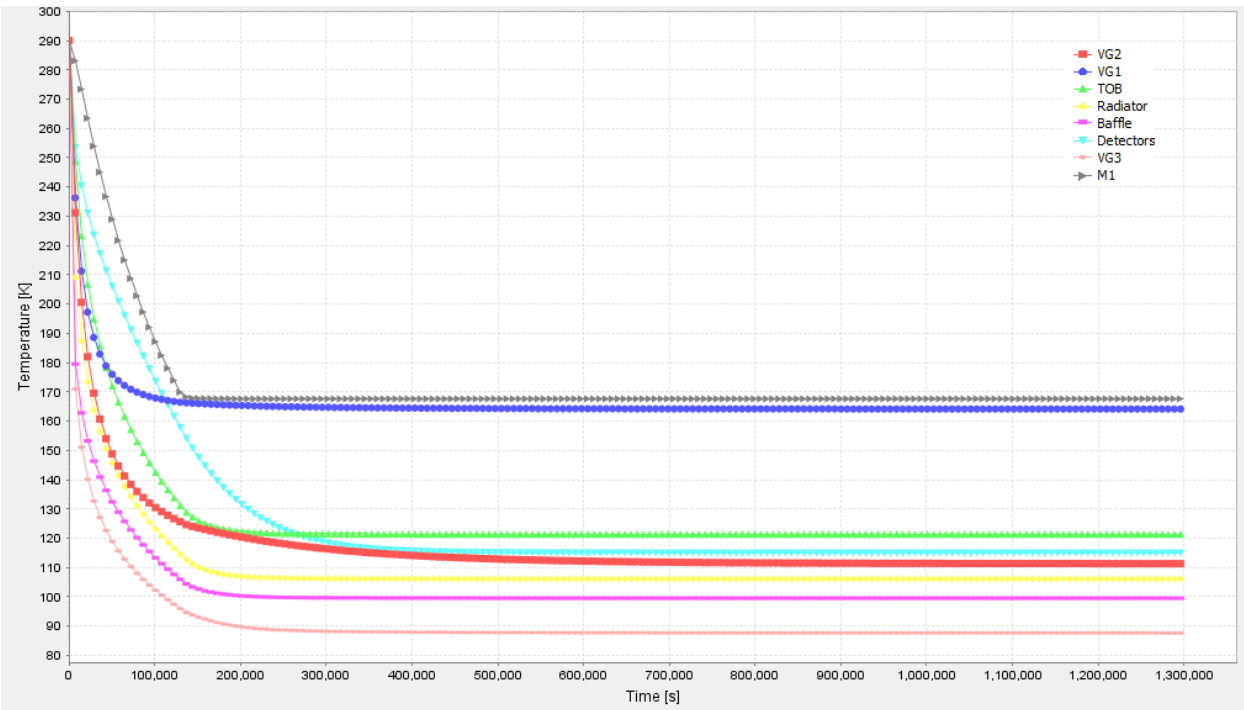


***Figure 34: PLM cool down simulation (15 days) with a heater on the Mirror 1 controlled by a PID element, for decontamination process.***

A more realistic cool-down transient simulation is then computed: in this case, once the M1 reaches 170 K, the heater on the M1 is turned on. The power supplied by the heater(s) at one of the central nodes of the M1 is controlled by a PID loop working only with proportional gain. The PID measures the temperature of this node and regulate the control power to the mirror center. Figure 34 shows the transient simulation for 15 days (1296000 s). Once the M1 reaches 170 K its temperature is stabilized by the proportionally controlled heater. As expected, the baffle, the radiators and the optical bench stabilize to much colder temperatures, at which the water can be condensed. Figure 35 shows the power dissipated by the heater vs time during the full transient simulation.

The average power value is around 26 W (40 W with 50 % margin).

## 4.2 LEOP THERMAL CASE

### 4.2.1 LEOP Steady-state analyses

The steady-state analysis in this case is used to identify the worst cases among all possible Sun vector orientations when solar radiation hits the PLM directly. Table 30 reports the solved steady-state temperatures for each considered Sun vector at LEOP scenario. The only boundary condition applied in this analysis in all these cases is the SVM top plate at 290 K, as a worst case temperature value.

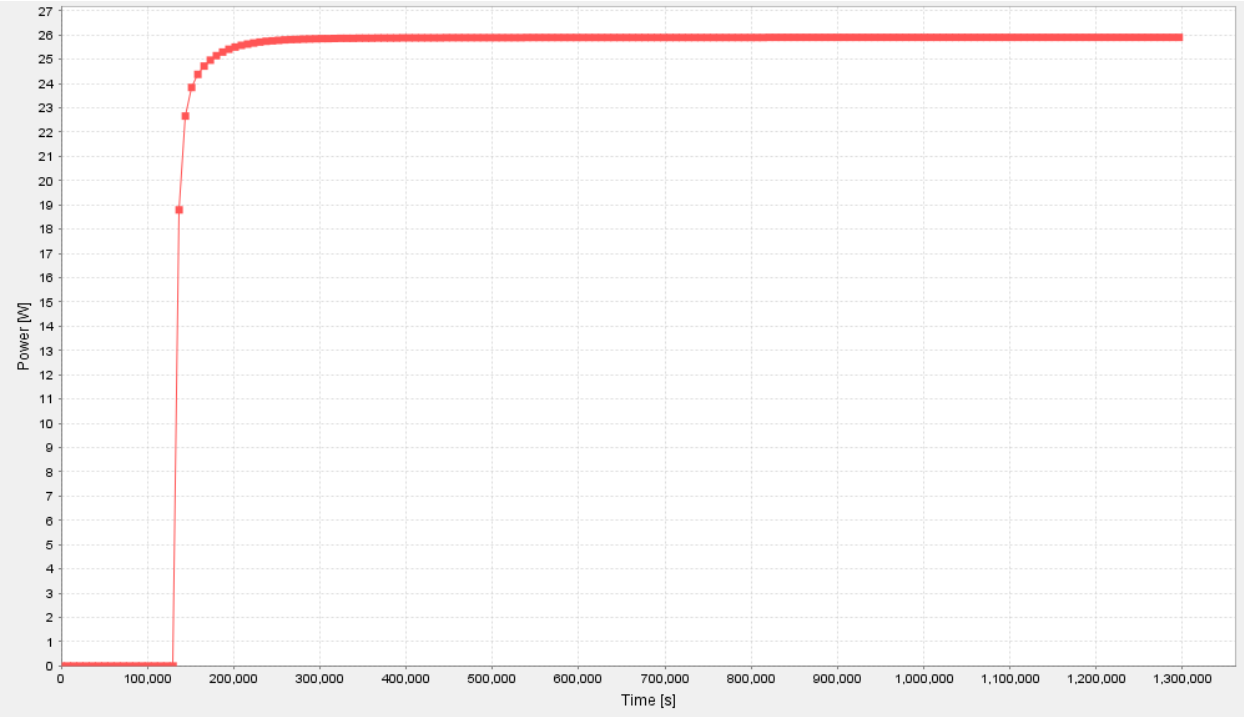


***Figure 35: Power dissipated by the heater on the M1 during decontamination process.***

If the main concern is related to the detectors and electronics maximum temperature that may be reached in such conditions, then the worst case Sun vector (see Table 30, temperatures are in Kelvin) is the one in $XZ_{ARIEL}$ plane with an angle of 115° from the $+X_{ARIEL}$ axis, that is basically tangent to the rear-side red cone (see Figure 18). In this case the Sun hits directly the optical bench, and in particular the instrument radiator that are exposed to the solar radiation. This Sun vector is assumed as the worst case condition and then used for the transient analysis.

***Table 30: Steady-state temperature results for different Sun vectors during LEOP.***

| | **Sun vector** | | | | | | |
|---|---|---|---|---|---|---|---|
| | In the $XZ_{ARIEL}$ plane, angle from the $+X_{ARIEL}$ axis: | | | | | In the $YZ_{ARIEL}$ plane, angle from the $+Y_{ARIEL}$ axis: | |
| | 65° | 90° | 95° | 100° | **115°** | 65° | 80° |
| | **Temperature [K]** | | | | | | |
| AIRS detectors | 301.4 | 329.4 | 335.7 | 342.0 | **355.2** | 327.1 | 329.9 |
| FGS detectors | 265.5 | 310.7 | 321.9 | 333.1 | **356.4** | 305.4 | 309.8 |
| AIRS CFEEs | 301.3 | 329.5 | 336.0 | 342.2 | **355.6** | 327.2 | 329.9 |
| FGS CFEEs | 300.0 | 328.7 | 335.3 | 341.8 | **355.6** | 325.3 | 328.7 |
| M1 | 322.6 | 338.4 | 341.2 | 343.6 | **346.4** | 333.6 | 338.0 |
| M2 | **390.6** | **376.2** | **367.9** | **363.7** | **327.7** | 368.8 | 376.0 |
| Instrument radiator | 258.3 | 308.5 | 337.7 | 332.8 | **358.0** | 303.9 | 308.2 |

| | | | | | | | |
|---|---|---|---|---|---|---|---|
| TOB | 305.7 | 331.8 | 321.3 | 343.3 | **353.9** | 328.3 | 331.9 |
| Baffle | 349.4 | 347.7 | 345.5 | 342.9 | **330.5** | 342.4 | 347.3 |
| VG3 | 365.5 | 369.7 | 368.1 | 366.1 | **356.2** | 361.0 | 368.4 |
| VG2 | 329.4 | 335.0 | 334.7 | 333.5 | **328.1** | 331.4 | 333.9 |
| VG1 | 323.7 | 327.1 | 329.3 | 327.5 | **322.1** | 330.7 | 328.9 |
| SVM Radiative shield | 317.8 | 316.4 | 321.4 | 318.2 | **315.6** | 325.7 | 321.3 |

In all Sun vector orientations analyzed, the secondary mirror M2 seems to reach temperatures regularly higher (20 to 30K) than the other units (Table 30). This is due to the fact that in the G/TMM there is no baffle covering the M2 (that was added later in the CAD). Moreover the M2 back side is assumed black painted to maximize radiative coupling to space. In the present telescope assembly configuration the thermo-optical properties of the M2 back side may be reviewed. In summary, this is not a realistic result: the actual final temperatures will be definitively lower because the M2 baffle will protect the mirror.

When the Sun vector enters on the PLM side (parallel to YZ plane), as expected, the last V-Groove and the Baffle pay the highest price while the module channels equilibrate to temperatures 25° C lower than worst case. The specifications for materials, coatings and processes for all PLM units shall be reviewed taking these possible conditions into account in the future design phase.

### 4.2.2 LEOP worst case transient analysis

Once the worst case Sun vector is identified it is possible to run a transient analysis to verify more realistically, even if in worst case conditions, the dynamical behavior of the units exposed to solar illumination. In this case the PLM is suddenly exposed to the worst case Sun vector (on $XZ_{ARIEL}$ plane with an angle of 115° from the $+X_{ARIEL}$ axis) for the expected duration of the process. The present issue of the Mission Analysis Guideline document [AD4] indicates a possible maximum exposition to Sun vectors in the allowed zone for a time of 37 minutes + TBD minutes. The transient simulation is then run for 1 hour, including some a margin to the given exposure time. The Sun vector direction is maintained fixed for the whole duration of the simulation (again, worst case condition). The initial temperature of all nodes is 290 K, the SVM top plate is kept at the fixed boundary temperature of 290 K. Figure 36 shows the temperature evolution of PLM units of 1 hour simulation.

***Table 31: Transient final temperature after 1 hour exposure to the worst case Sun vector.***

| Unit | T [K] | T [C] |
|---|---|---|
| AIRS detectors | 290.4 | 17.3 |
| FGS detectors | 335.0 | 61.9 |
| AIRS CFEEs | 321.3 | 48.2 |
| FGS CFEEs | 313.2 | 40.1 |
| M1 | 292.5 | 19.4 |
| M2 | 311.5 | 38.4 |
| Instrument radiator | 342.0 | 68.9 |
| TOB | 315.6 | 42.5 |
| Baffle | 322.8 | 49.7 |
| VG3 | 350.4 | 77.3 |
| VG2 | 310.6 | 37.5 |
| VG1 | 306.9 | 33.8 |
| SVM Radiative shield | 296.6 | 23.5 |

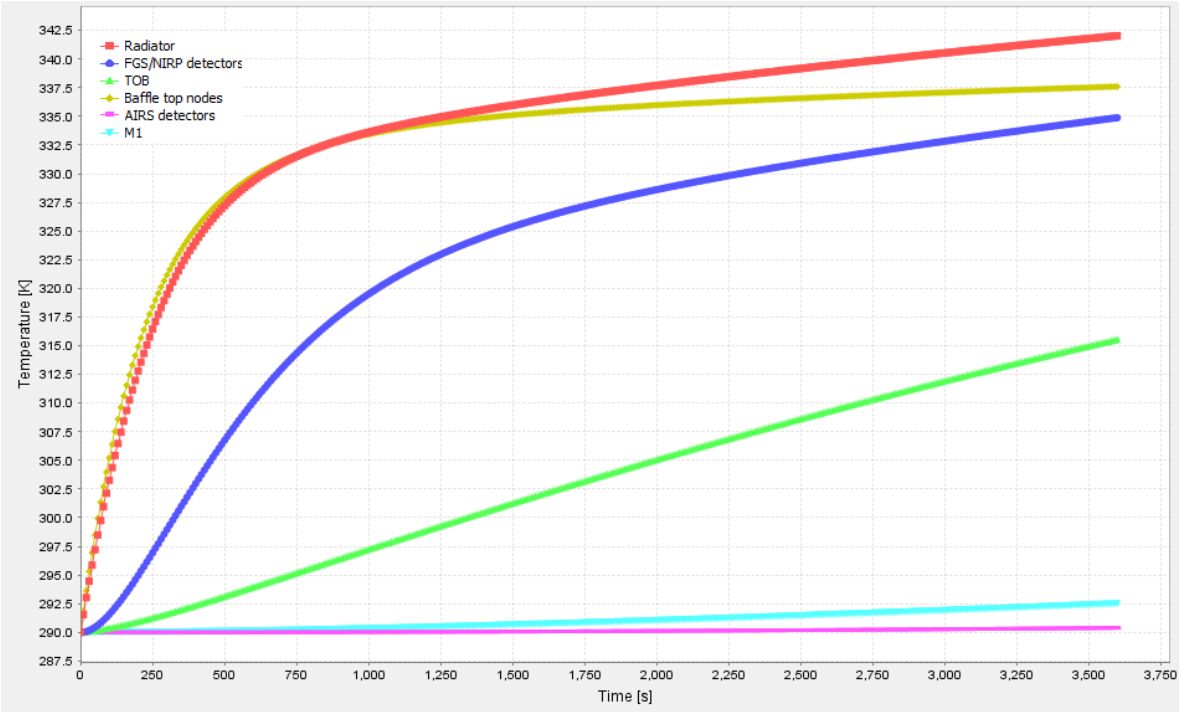


***Figure 36: Transient solution for 1 hour exposure of the PLM to the worst case Sun vector.***

Table 31 reports the final transient temperatures of the main PLM units after 1 hour exposure to the worst case Sun vector.

As expected, the FGS/NIRP detectors temperature follows a fast steep ramp up to its maximum value as these FPA's are directly coupled to the instrument radiator which is exposed to the solar rays. The AIRS detectors temperature, on the other side, runs almost unperturbed at least for these first 60 minutes. This is due to the fact that the AIRS FPA's are well insulated from the bench and the combination of this high resistance with the thermal inertia of the OB itself and of their module box results in a long time constant. We know (see Figure 30) that at steady state the AIRS detectors will end up to the same temperature of the other SCA's but this happens in a time scale much longer than 1 hour, keeping the detectors at a safe temperature for such durations of the exposure.

Before changing the thermo-optical design of the PLM units, a possible way to solve or, at least, mitigate the issue of the high temperatures that can be reached in case of Sun intrusion, is to adjust thermal resistances and capacitances of the subsystems involved. By slightly increasing the thermal inertia of each unit, it is possible to slow down all temperature changes. If an increased mass, a slightly higher operating temperature or a slower cool-down time can be accepted with sufficient margin, then a set of simulations can be run to estimate the tuning level needed on capacitances and resistances to implement a safer design.

# 5 SUMMARY AND CONCLUSIONS

The thermal model results, heat fluxes across the interfaces and units temperature, indicate a reliable PLM thermal architecture, compliant to the requirement including the present level of margin. The next steps of the thermal analysis will be aimed to reach a higher level of detail, to optimize the design and to prepare a more reliable assessment of uncertainties and margins at the interfaces.

## 5.1 ARIEL PLM UNITS TEMPERATURE PREDICTIONS

In Figure 37 the operating temperature ranges from Cold to Hot Case of the main PLM units are reported as grey boxes. These boxes are shown in the picture together with the requirements (blue bars) plus the margins (yellow bars) required by the present level of the design.

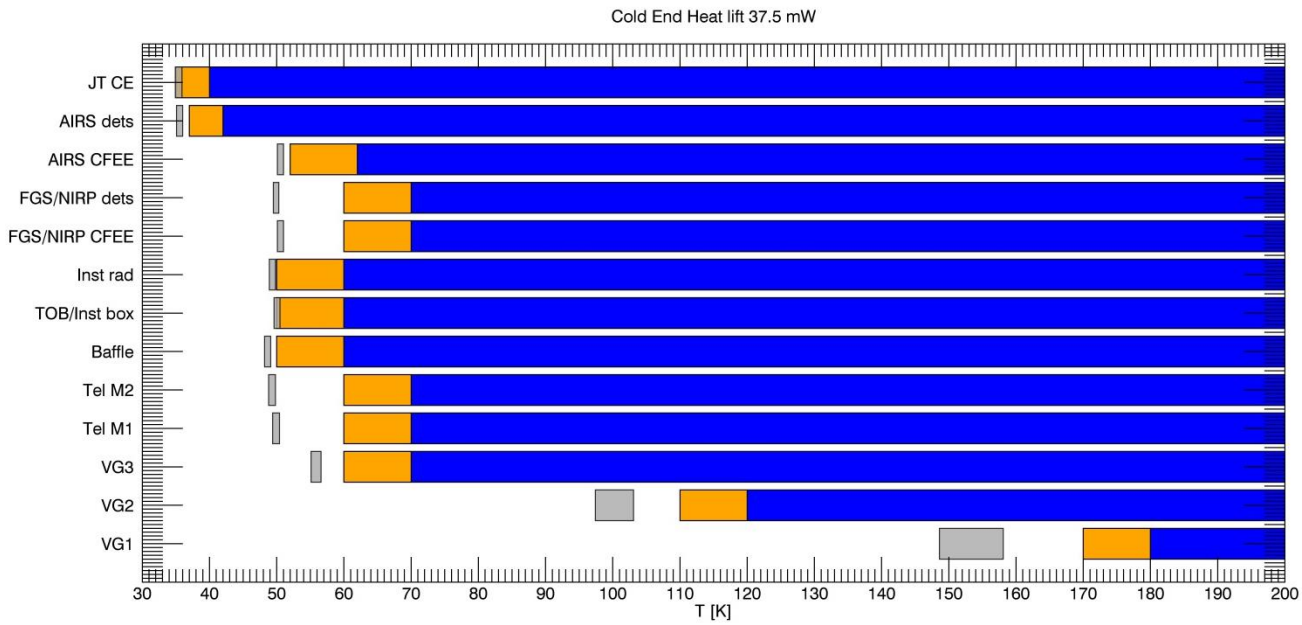


***Figure 37: Main PLM units temperature in Cold and Hot case are compared to the requirement (blue bars) with margins (yellow bars)***

For both thermal cases, all temperatures result below, or at, the required values including margin, indicating a fully compliant thermal architecture with some extra space for further optimizations. In phase B1 the thermal architecture will be optimized to reduce the uncertainty margins and increase the design margins on the passive and active cooling stages, especially the coldest ones.

## 5.2 THERMAL BUDGETS

The ARIEL PLM loads, especially for what concerns detectors dissipation, mechanical supports, piping and harness leaks, have been evaluated on the basis of the present knowledge of the units performances and of the heritage from more advanced projects (MIRI, Planck, Euclid etc.). Conservative estimations have been assumed and verified by thermal analysis with the PLM G/TMM.

The budget resulting at the external thermal interface and at the main six internal interfaces from the analysis activity is reported in Table 32 and Table 33. The values correspond to the loads calculated by the TMM in the two main reference cases: Cold and Hot. The fact that the heat fluxes reported in Table 33 correspond to interface temperatures lower than required, indicate that extra margin is available for optimizations in the next phase.

*Table 32: ARIEL external thermal interface budget*

| External Interface | Location | IF to | Req T [K] | Cold Case T [K] | Cold Case Load [mW] | Hot Case T [K] | Hot Case Load [mW] |
|---|---|---|---|---|---|---|---|
| **TIF0** | **SVM Conducted** | **Bipods and VG struts** | **≤ 290** | **270** | **-6040** | **290** | **-8720** |
| | **SVM Radiative** | **VG1 (mainly)** | **≤ 290** | **180** | **-1430** | **200** | **-2460** |

*Table 33: ARIEL internal thermal interfaces budget*

| Internal Interface | Location | IF to | Req T [K] | Cold Case T [K] | Cold Case Load [mW] | Hot Case T [K] | Hot Case Load [mW] |
|---|---|---|---|---|---|---|---|
| TIF1 | V-Groove 1 | Heat leaks from SVM (harness, bipods, struts, piping, radiation) | ≤ 200 | 149 | 7470 | 158 | 11180 |
| TIF2 | V-Groove 2 | Heat leaks from warmer stages (harness, bipods, struts, piping, radiation) | ≤ 120 | 97 | 1130 | 103 | 1400 |
| TIF3 | V-Groove 3 | Heat leaks from warmer stages (harness, bipods, struts, piping, radiation) + JT precooling | ≤ 70 | 55 | 980 | 57 | 1100 |
| TIF4 | TOB/Baffle | Channels FEE, parasitics, rad | ≤ 60 | 50 | 740 | 51 | 810 |
| TIF5 | Instrument Radiator | FGS/NIRP detectors + T control stage loads + parasitic leaks | ≤ 60 | 49 | 100 | 50 | 100 |
| TIF6 | JT cold end | AIRS detectors + T control stage loads + parasitics leaks (struts+harness+rad) | < 40 | 35 | 37.5 | 36 | 37.5 |

# 6 UNCERTAINTY ANALYSIS

A preliminary uncertainty analysis has been performed with the PLM TMM in order to assess the uncertainties of the design and possibly increase the already positive margin above the standard 10K and 5K that must be assumed on passive and active cooling design. The thermal engineering design driver for the ARIEL PLM is “the colder, the better”. Having this principle in mind, safe margins on conductances and loads have been used throughout the analysis in order to have a worst case scenario in all thermal cases.

A summary list of the uncertainties considered in the ARIEL PLM model is:

- Active dissipation: even if the active units design in the ARIEL PLM is derived from the heritage on other projects (used and/or measured), a margin of 30 to 50% has been applied to all loads as a worst case
    - Thermal conductivity (see next paragraph):
    - Metallic materials +/-15%
- GFRP +/-30%
- Harness: the cables design and thermal properties have been derived from previous projects, but given the preliminary assumptions made on routing and configuration, a 50 % margin has been assumed
- Contact resistance: +/-50%
- Emissivity:
    - High emissivity (>0.2): +/-0.03
    - Low emissivity (<0.2): +/-0.02
- Interface temperature ranges: as the only external interface is with the SVM platform, an worst case uncertainty of +5K has been assumed on its highest temperature (290K)
- Uncertainties on aging effects: at this stage aging effects have been assumed only on thermo-optical properties and their possible variations are assumed to be included in the uncertainty on emissivity

## 6.1 CONDUCTIVITY

All materials properties used in the PLM thermal design have been assumed on the basis of the best cryogenic databases, heritage from previous applications and technical papers. Common materials (like Al alloys), used frequently in the past, show a high number of measured data sources and can benefit from their use in previous projects, that help in decreasing the uncertainty. For less common materials such as GFRP, at low T especially, a higher uncertainty must be assumed.

***Table 34. Assumed uncertainty on materials thermal conductivity***

| Material | Conductivity uncertainty [%] |
|---|---|
| Al6061 | ± 15 |
| GFRP | ± 30 |
| Ti6Al4V | ± 100 |

## 6.2 EMISSIVITY

Assumptions on the IR emissivity of the ARIEL PLM units have been made on the basis of previous experiences and know materials properties.

***Table 35. Max and min values used for the sensitivity analysis on the emissivity***

| Units | IR emissivity | | |
|---|---|---|---|
| | **Max** | **Min** | **Nominal Case** |
| Black paint | 0.93 | 0.87 | 0.9 |
| Black painted Open honeycomb | 0.93 | 0.87 | 0.9 |
| Reflective surfaces VG | 0.07 | 0.03 | 0.05 |
| Reflective surfaces mirrors | 0.02 | 0.70 | 0.02 |
| Instrument Cavity/ metallic surfaces | 1.00 | 1.00 | 1.00 |

All the parameters variations assumed for this analysis are based on the present estimation of knowledge of instrument design and materials and on ECSS indications.

## 6.3 UNCERTAINTY ANALYSIS RESULTS

Simulation runs have been completed with the max and min values reported in the tables above to assess the main units sensitivity to each parameter. The impact of changing single parameters values within the max and min uncertainty range on the PLM thermal architecture design seems minor and not immediately evident. For this reason, a single worst case analysis has been run in order to evaluate the model results with all parameters uncertainties combined together. This simulation has been performed assuming for each uncertainty the extreme value that maximise the final temperature of the PLM units, as this is the worst, and realistic, case to verify the ARIEL thermal design sensitivity to the maximum uncertainties. Table 36 reports the uncertainty values for each parameter used for the worst case run.

***Table 36: Parameters modified in the uncertainty analysis***

| | |
|---|---|
| Al6061 conductivity | - 15% |
| GFRP conductivity | + 30% |
| Ti6Al4V | + 100% |
| Contact conductance Bipods/SVM top plate | + 50% |
| Black paint emissivity | 0.87 |
| SVM MLI emissivity | 0.07 |
| VDA emissivity | 0.07 |
| Pre-cooling loop power load on VG3 | 500 mW |
| Cold case SVM top plate temperature | 265 K |
| Hot case SVM top plate temperature | 295 K |

The results are reported in the Table 37. Max Uncertainties Cold and Hot cases are compared to the results with Nominal assumptions. The temperatures of some stages or units are up to 3 – 4 K higher than Nominal cases but still below the requirements including, in most cases, the uncertainty margin.

***Table 37. Steady-state temperatures for the cold and hot case in worst case uncertainty conditions.***

| | **Nominal Cold case T [K]** | **Max Uncertainty Cold case T [K]** | **Nominal Hot case T [K]** | **Max Uncertainty Hot case T [K]** |
|---|---|---|---|---|
| *SVM top plate (fixed boundary temperature)* | *270.00* | *265.00* | *290.00* | *295.00* |
| *SVM Radiative shield (fixed boundary* | *180.00* | *180.00* | *200.00* | *200.00* |

| | | | | |
|---|---|---|---|---|
| *temperature)* | | | | |
| VG1 | 148.6 | 147.6 | 158.1 | 160.2 |
| VG2 | 97.4 | 100.5 | 103.1 | 108.6 |
| VG3 | 55.1 | 59.1 | 56.6 | 61.4 |
| Telescope M1 | 49.4 | 52.3 | 50.4 | 53.9 |
| Telescope M2 | 48.8 | 51.7 | 49.8 | 53.4 |
| Telescope Baffle | 48.2 | 50.9 | 49.1 | 52.5 |
| TOB | 49.6 | 52.5 | 50.5 | 54.0 |
| Instrument Box | 49.6 | 52.5 | 50.5 | 54.1 |
| FGS/NIRP CFEEs | 50.1 | 53.0 | 51.0 | 54.5 |
| FGS/NIRP detectors | 49.5 | 52.2 | 50.3 | 53.7 |
| Instrument radiator | 48.9 | 51.6 | 49.8 | 53.2 |
| AIRS CFEEs | 50.1 | 53.0 | 51.0 | 54.6 |
| AIRS detectors | 35.1 | 38.0 | 36.0 | 39.6 |
| JT cold end | 34.9 | 37.9 | 35.9 | 39.4 |

# 7 ACKNOWLEDGMENTS

We acknowledge the financial contribution by the Italian Space Agency to the ARIEL project in the framework of the ASI-INAF agreement 2015-038-R.0.

# 8 APPENDIX: G/TMM FILE NAME AND CONTENT

The ARIEL PLM G/TMM is compressed in the ARIEL-INAF-PL-ML-002.zip file.

The zip file includes:

- A ***pdf*** file describing the content of the ***.zip***, down to the sub-folders
- The GMM in the ***.erg*** file
- A sub-folder for each analysis case, containing the corresponding input file ***.d*** and the output file ***.out***